

# STOPPING CRITERIA FOR THE CONJUGATE GRADIENT ALGORITHM IN HIGH-ORDER FINITE ELEMENT METHODS \*

YICHEN GUO<sup>†</sup>, ERIC DE STURLER<sup>†</sup>, AND TIM WARBURTON<sup>†</sup>

**Abstract.** We introduce three new stopping criteria that balance algebraic and discretization errors for the conjugate gradient algorithm applied to high-order finite element discretizations of Poisson problems. The current state of the art stopping criteria compare a posteriori estimates of discretization error against estimates of the algebraic error. Firstly, we propose a new error indicator derived from a recovery-based error estimator that is less computationally expensive and more reliable. Secondly, we introduce a new stopping criterion that suggests stopping when the norm of the linear residual is less than a small fraction of an error indicator derived directly from the residual. This indicator shares the same mesh size and polynomial degree scaling as the norm of the residual, resulting in a robust criterion regardless of the mesh size, the polynomial degree, and the shape regularity of the mesh. Thirdly, in solving Poisson problems with highly variable piecewise constant coefficients, we introduce a subdomain-based criterion that recommends stopping when the norm of the linear residual restricted to each subdomain is smaller than the corresponding indicator also restricted to that subdomain. Numerical experiments, including tests with anisotropic meshes and highly variable piecewise constant coefficients, demonstrate that the proposed criteria efficiently avoid both premature termination and over-solving.

**Key words.** stopping criteria, high-order finite element method, conjugate gradient algorithm,  $p$ -robust

**MSC codes.** 65N30, 65N22, 65F10

**1. Introduction.** Solving linear elliptic partial differential equations (PDEs) involves two main steps: discretization of the PDE and solving the resulting algebraic linear system. As a result, two primary sources of error emerge: discretization error and algebraic error, which results from the iterative solution of the linear system. The efficient termination of iterative solvers achieves a balance between discretization error and algebraic error. Ideally, a stopping criterion for the iterative solver suggests stopping the iteration when the algebraic error is dominated by the discretization error. A desirable stopping criterion should be reliable in the sense of maintaining the overall accuracy of the finite element solution, and efficient in the sense of terminating the iterative solver as early as possible. Moreover, the criterion should be inexpensive to compute and the computation should be memory efficient. In this paper, we consider the Poisson problem discretized with high-order finite element methods (FEM), and we solve the linear system using the Conjugate Gradient algorithm (CG). For this study, we assume the finite element space has already been fixed, and we aim to iterate until the error due to the given discretization dominates the error due to the linear system.

The design of stopping criteria in finite element frameworks has been explored in numerous papers [2, 5, 36, 24, 4, 19, 3, 33]. One commonly adopted criterion in these works involves assessing when the ratio of estimated algebraic error to the estimated total error falls below a threshold. Algebraic error estimation was discussed early on by Hestenes and Stiefel in [23], and further developed in [21, 29, 28, 27, 22]. It is common for this type of algebraic error estimation to rely on computing the difference between the computed solutions at two different iterations with a heuristically chosen gap between the iterations. If the iterative convergence rate is slow, then a larger delay (i.e. a greater number of additional iterations) may be necessary. As indicated by numerical experiment 4.1.2 presented in [2], it can be challenging to determine a reliable delay parameter for the Poisson problem with a highly variable coefficient, due to the potential need to use a large delay to compensate for slow iterative convergence.

Monitoring the total error in finite element methods is also a key ingredient when devising stopping criteria. In the context of our study, we refer to an error indicator as an “error

\*Submitted to the editor May 12 2023.

**Funding:** This work was supported under NSF DMS 2208470. The third author was supported in part by the Exascale Computing Project, a collaborative effort of two U.S. Department of Energy organizations (Office of Science and the National Nuclear Security Administration) responsible for the planning and preparation of a capable exascale ecosystem, including software, applications, hardware, advanced system engineering, and early testbed platforms, in support of the nation’s exascale computing imperative. He was also supported in part by the John K. Costain Faculty Chair in Science at Virginia Tech. The first author acknowledges the generous support from the John K. Costain Graduate Fellowship.

<sup>†</sup>Department of Mathematics, Virginia Tech, Blacksburg, VA 24061 (ycguo@vt.edu, sturler@vt.edu, tcew@vt.edu)

estimator” if it is equivalent to the exact total error. Specifically, an error estimator should provide both upper and lower bounds to the total error up to a constant independent of the polynomial degree and the mesh size. Babuška and Rheinboldt [8] proposed a residual-based a posteriori error estimator for low-order FEM on one-dimensional domains in the late 1970s. Subsequently, Melenk and Wohlmuth [25] extended the estimator for  $hp$ -FEM by generalizing the Clément interpolation operator to the  $hp$ -finite element discretization. However, their estimator is an upper bound for the error only up to an unknown constant that depends on the shape regularity of the triangulation, which may lead to a significant overestimation of the error. Methods for estimating the unknown constant, as developed in [16, 40], require solving local eigenvalue problems, or obtaining trace inequalities and Poincaré-type inequalities with explicit constants. On the other hand, flux recovery error estimation techniques [10, 9, 43, 13] introduced in [44, 45] reconstruct an approximation to the flux and compare the reconstructed flux with the numerical flux. The efficiency of this approach is robust with respect to the polynomial degree; however, solving this requires a significant amount of computation and memory for high-order finite element approximation. Our goal is to design a reliable and efficient stopping criterion that is also robust with respect to the mesh size, the polynomial degree, the shape regularity of the mesh, and the diffusion coefficient. To design such a stopping criterion, we propose three main innovations. Firstly, as for stopping criteria based on a comparison of the algebraic error estimator and the a posteriori error estimator [2, 36, 19, 3], we propose an alternative error indicator that serves as a lower bound for the recovery-based error estimator, using the singular value decomposition of elliptic lifting matrices arising from local problems in flux recovery. The indicator is computationally less expensive to evaluate while iterating and more reliable than the recovery-based error estimator for high-order elements.

Secondly, in contrast to criteria comparing error estimates, we propose a simplified stopping criterion that depends on the norm of the linear residual and an error indicator for the Poisson problem with a constant diffusion coefficient. We decompose the linear residual into a component corresponding to the strong residual tested against the basis functions and a second component corresponding to the jumps in the normal gradient at element interfaces also tested against the basis functions. We then apply the triangle inequality to derive an error indicator that is directly comparable to the norm of the linear residual. This indicator tends to stagnate when the discretization error dominates the algebraic error, as it depends on the strong residual and jumps in the normal gradient. Therefore, the divergence of this indicator from the norm of the linear residual can be an effective proxy for identifying when the discretization error dominates the algebraic error. This observation motivates a criterion for terminating the iterative method when the ratio of the norm of the linear residual to the new indicator falls below a specific tolerance. The proposed indicator is a natural upper bound for the norm of the residual without any unknown constants to be estimated. It has the same intrinsic mesh size and polynomial degree scaling as the norm of the linear residual, which coincides with the scaling of the energy norm of the error in two dimensions. Moreover, compared with criteria based on error estimation, the proposed criterion does not require estimating the algebraic error since it relies on the linear residual. Furthermore, separate computation of the component corresponding to jumps in the normal gradient is unnecessary, as it can be obtained directly from the difference between the linear residual and the component corresponding to the strong residual. By contrast, both strong element residuals and jump residuals are computed in residual a posteriori estimators [8, 25].

Finally, it is important to note that the diffusion coefficient scaling in the norm of the linear residual and the new indicator is different from the scaling in the total error for problems with highly variable diffusion coefficient. This implies that contributions from subdomains with small coefficients may be dominated by contributions from subdomains with large coefficients. Thus, when solving the Poisson equation with highly variable coefficients, the separation of the indicator and the norm of the linear residual may occur at a different iteration than the point at which the discretization error dominates over the algebraic error. To address this issue, we propose a subdomain-based criterion that only recommends stopping when the norm of the linear residual restricted to each subdomain is relatively small compared to the indicator restricted to that subdomain. This approach ensures that the iteration achieves sufficient accuracy in all subdomains and provides a reliable stopping criterion for problems with highly variable piecewise constant coefficients.

The paper is organized as follows. In section 2, we review stopping criteria based on a comparison of estimates of the algebraic error and a posteriori estimates of discretization error for high-order finite element methods. Additionally, we propose an error indicator. In section 3, we introduce a new stopping criterion that compares the norm of the residual and an indicator, and a subdomain-based stopping criterion for problems with highly variable coefficients. In section 4, we provide numerical results to demonstrate the effectiveness of the stopping criteria. Numerical experiments include tests with anisotropic meshes, solutions with singularities, and Poisson problems with highly variable piecewise constant coefficients. We end with conclusions in section 5.

Throughout this paper, we will use standard notation from Sobolev space theory. For a bounded domain  $\Omega \subset \mathbb{R}^d$ ,  $(\cdot, \cdot)$  and  $\|\cdot\|_\Omega$  denote the inner product and the associated norm on  $L^2(\Omega)$ . For a vector  $\mathbf{x} \in \mathbb{R}^n$ ,  $\|\mathbf{x}\|$  denotes the  $l^2$  norm of  $\mathbf{x}$ .

**2. Formulation.** We consider the Poisson problem

$$(2.1) \quad -\nabla \cdot (\kappa(x) \nabla u(x)) = f(x)$$

on a bounded domain  $\Omega \subset \mathbb{R}^d$ , with boundary conditions

$$\frac{\partial u}{\partial n} = g \text{ on } \Gamma_N, \quad u = 0 \text{ on } \Gamma_D,$$

where  $\Gamma_N \cap \Gamma_D = \emptyset$ ,  $\bar{\Gamma}_D \cup \bar{\Gamma}_N = \partial\Omega$ ,  $f \in L^2(\Omega)$ , and  $g \in L^2(\Gamma_N)$  describes the Neumann boundary condition. We assume there exists a constant  $\alpha$  such that  $0 < \alpha \leq \kappa(x) \in L^2(\Omega)$ .

We define  $H_{0,\Gamma_D}^1(\Omega) := \{v \in H^1(\Omega) : v|_{\Gamma_D} = 0\}$ . The weak formulation of the Poisson equation (2.1) is: find  $u \in H_{0,\Gamma_D}^1(\Omega)$ , such that

$$(2.2) \quad a(u, v) = \ell(v), \quad \forall v \in H_{0,\Gamma_D}^1(\Omega),$$

where

$$\begin{aligned} a(u, v) &:= \int_{\Omega} \kappa(x) \nabla u \cdot \nabla v \, dx, \quad u, v \in H_{0,\Gamma_D}^1(\Omega), \\ \ell(v) &:= \int_{\Omega} f v \, dx + \int_{\Gamma_N} g v \, ds, \quad v \in H_{0,\Gamma_D}^1(\Omega). \end{aligned}$$

We use the notation  $\|\cdot\|_E$  to denote the energy norm

$$\|v\|_E = \sqrt{a(v, v)}.$$

Given a family of regular affine triangulations  $\mathcal{T}_h = \{K\}$  of  $\Omega$  with elements  $K$ , we define the finite element space  $S_N(\mathcal{T}_h, \Omega)$  of piecewise polynomials of degree  $N$

$$S_N(\mathcal{T}_h, \Omega) := \{v_h \in H_{0,\Gamma_D}^1(\Omega) : v_h|_K \in \mathbb{P}_N(K), K \in \mathcal{T}_h\}.$$

We denote by  $\mathbb{P}_N(K)$  the linear space of polynomials of total degree  $\leq N$  on  $K$ , by  $N_s$  the dimension of  $S_N(\mathcal{T}_h, \Omega)$ , and by  $\phi_n$  basis functions of  $S_N(\mathcal{T}_h, \Omega)$ , where  $n = 1, \dots, N_s$ . In this work  $\phi_n$  denotes the Lagrange interpolating basis function associated with the  $n$ -th node of the degree  $N$  Warp & Blend nodes for the triangle [42]. We refer to  $\mathcal{E}$  as the set of all  $(d-1)$ -dimensional element edges (faces in  $\mathbb{R}^3$ ) of  $\mathcal{T}_h$ . Furthermore, we define  $\mathcal{E}_{\text{bd}}$  as the set of element edges that lie on  $\Gamma_N$ , and decompose  $\mathcal{E}$  into  $\mathcal{E}_{\text{bd}}$  and  $\mathcal{E}_{\text{int}} = \mathcal{E} \setminus \mathcal{E}_{\text{bd}}$ . The finite element approximation to (2.1) is: find  $u_h \in S_N(\mathcal{T}_h, \Omega)$  such that

$$(2.3) \quad a(u_h, v) = \ell(v), \quad \forall v \in S_N(\mathcal{T}_h, \Omega).$$

Equations (2.2) and (2.3) give rise to the Galerkin orthogonality condition

$$(2.4) \quad a(u - u_h, v) = 0 \quad \forall v \in S_N(\mathcal{T}_h, \Omega).$$

The approximation problem (2.3) is equivalent to the linear system:

$$(2.5) \quad \mathbf{Ax} = \mathbf{b},$$

where  $\mathbf{A} \in \mathbb{R}^{N_s \times N_s}$  and  $\mathbf{b} \in \mathbb{R}^{N_s}$  are defined as follows,

$$\mathbf{A}_{ij} = a(\phi_j, \phi_i), \quad \mathbf{b}_i = \ell(\phi_i).$$

The matrix  $\mathbf{A}$  is symmetric and positive definite. We define the  $\mathbf{A}$ -norm of  $\mathbf{x}$  as  $\|\mathbf{x}\|_{\mathbf{A}} = (\mathbf{x}^T \mathbf{A} \mathbf{x})^{1/2}$ . We assume that  $\mathbf{x}_k \in \mathbb{R}^{N_s}$  is an approximate solution to (2.5) obtained by an iterative method at the  $k$ -step, which in turn provides an approximate finite element solution  $u_h^k = \sum_{i=1}^{N_s} x_i^k \phi_i$ . The total error, the discretization error, and the algebraic error are denoted by

$$e := u - u_h^k, \quad e_{\text{dis}} := u - u_h, \quad e_{\text{alg}} := u_h - u_h^k,$$

respectively. From the relation  $a(e_{\text{alg}}, e_{\text{alg}}) = (\mathbf{x} - \mathbf{x}_k)^T \mathbf{A} (\mathbf{x} - \mathbf{x}_k)$ , we have

$$(2.6) \quad \|e_{\text{alg}}\|_E = \|\mathbf{x} - \mathbf{x}_k\|_{\mathbf{A}}.$$

The Galerkin orthogonality condition (2.4) implies

$$\|e\|_E^2 = \|e_{\text{dis}}\|_E^2 + \|e_{\text{alg}}\|_E^2.$$

As the iteration proceeds, the algebraic error gradually approaches zero, leading the total error to converge to the discretization error. Ideally, the iteration is terminated when the discretization error is dominant in the total error, i.e.,

$$(2.7) \quad \|e_{\text{alg}}\|_E \leq \tau \|e\|_E,$$

for a chosen tolerance  $\tau$ , where  $0 < \tau < 1$ . Since the total error and the algebraic error are unknown in general, we use error estimators  $\eta_{\text{alg}}$  and  $\eta_{\text{tot}}$  to estimate the energy norm of the algebraic error,  $\|e_{\text{alg}}\|_E$ , and the total error,  $\|e\|_E$ , respectively. We review estimation of the algebraic error for the conjugate gradient algorithm in subsection 2.1 and several discretization error estimators for high-order finite element methods in subsection 2.2.

**2.1. Error estimation for the conjugate gradient algorithm.** The conjugate gradient algorithm was introduced by Hestenes and Stiefel [23] in 1952, and they also proposed a method to estimate the error. In [39], Strakoš and Tichý showed that the estimation proposed in [23] is numerically stable. For the sake of completeness, we briefly discuss the conjugate gradient algorithm and the error estimator proposed in [23]. We use the error estimator of CG as the algebraic error estimator  $\eta_{\text{alg}}$  because of the equivalence of the  $\mathbf{A}$ -norm of CG error and the energy norm of the algebraic error (2.6). A comprehensive summary of CG is given in [26].

The conjugate gradient algorithm is as follows. Given  $\mathbf{x}_0$ ,  $\mathbf{r}_0 = \mathbf{b} - \mathbf{A}\mathbf{x}_0$ ,  $\mathbf{p}_0 = \mathbf{r}_0$ . For  $k = 1, 2, \dots$ ,

$$\begin{aligned} \gamma_{k-1} &= \frac{\|\mathbf{r}_{k-1}\|^2}{\|\mathbf{p}_{k-1}\|_{\mathbf{A}}^2}, & \mathbf{x}_k &= \mathbf{x}_{k-1} + \gamma_{k-1} \mathbf{p}_{k-1}, & \mathbf{r}_k &= \mathbf{r}_{k-1} - \gamma_{k-1} \mathbf{A} \mathbf{p}_{k-1}, \\ \beta_k &= \frac{\|\mathbf{r}_k\|^2}{\|\mathbf{r}_{k-1}\|^2}, & \mathbf{p}_k &= \mathbf{r}_k + \beta_k \mathbf{p}_{k-1}. \end{aligned}$$

The algorithm computes directions  $\mathbf{p}_i$  that are  $\mathbf{A}$ -orthogonal, i.e.  $\mathbf{p}_i^T \mathbf{A} \mathbf{p}_j = 0$ ,  $i \neq j$ . The approximate solution at the  $k$ -th step is

$$\mathbf{x}_k = \mathbf{x}_0 + \sum_{i=0}^{k-1} \gamma_i \mathbf{p}_i.$$

To illustrate the idea of the error estimation, we assume that the CG algorithm can be run for  $N_s$  steps and the exact solution  $\mathbf{x}$  satisfies

$$\mathbf{x} = \mathbf{x}_0 + \sum_{i=0}^{N_s} \gamma_i \mathbf{p}_i.$$

The  $\mathbf{A}$ -norm of the CG error is

$$\|\mathbf{x} - \mathbf{x}_k\|_{\mathbf{A}} = \left( \sum_{i=k}^{N_s} \gamma_i^2 \|\mathbf{p}_i\|_{\mathbf{A}}^2 \right)^{1/2}.$$

If the delay parameter  $d$  satisfies  $\|\mathbf{x} - \mathbf{x}_{k+d}\|_{\mathbf{A}} \ll \|\mathbf{x} - \mathbf{x}_k\|_{\mathbf{A}}$ , then as

$$\|\mathbf{x} - \mathbf{x}_k\|_{\mathbf{A}}^2 = \|\mathbf{x}_{k+d} - \mathbf{x}_k\|_{\mathbf{A}}^2 + \|\mathbf{x} - \mathbf{x}_{k+d}\|_{\mathbf{A}}^2,$$

Hestenes and Stiefel [23] estimate the  $\mathbf{A}$ -norm of the CG error  $\|\mathbf{x} - \mathbf{x}_k\|_{\mathbf{A}}$  by

$$(2.8) \quad \eta_{\text{alg}} := \|\mathbf{x}_{k+d} - \mathbf{x}_k\|_{\mathbf{A}}.$$

Hence, additional  $d$  iterations are required to compute the estimator at the  $k$ -th step.

It is challenging to choose  $d$  in advance, since the parameter depends on the convergence rate of CG. To achieve the same accuracy, the slower CG converges, the larger  $d$  has to be. If  $\alpha \|\mathbf{x} - \mathbf{x}_k\|_{\mathbf{A}}^2 = \|\mathbf{x} - \mathbf{x}_{k+d}\|_{\mathbf{A}}^2$  with  $\alpha \in (0, 1)$ , the effectivity of (2.8) is

$$\frac{\eta_{\text{alg}}}{\|\mathbf{x} - \mathbf{x}_k\|_{\mathbf{A}}} = (1 - \alpha)^{1/2}.$$

We demonstrate in section 4 that, with  $d = 10$ ,  $\eta_{\text{alg}}$  is a good estimator if the algebraic error decreases fast, while it is unsatisfactory for some problems where the error remains almost constant for a number of iterations. An increase in  $d$  improves the accuracy of the estimator; however, it also leads to an increased number of additional iterations, which is undesirable.

**2.2. Survey of A Posteriori error estimators.** In this subsection, we review error estimators based on the residual and flux reconstruction. To simplify notation, we define the element residual,  $r_E : \Omega \rightarrow \mathbb{R}$ , and the edge residual,  $r_J : \mathcal{E} \rightarrow \mathbb{R}$ , by

$$(2.9) \quad r_E|_K = f + \nabla \cdot (\kappa(x) \nabla u_h^k) \text{ in } K,$$

$$(2.10) \quad r_J|_{\ell} = \begin{cases} -[(\kappa(x) \nabla u_h^k) \cdot \mathbf{n}_{\ell}] & \text{if } \ell \in \mathcal{E}_{\text{int}}, \\ g - (\kappa(x) \nabla u_h^k) \cdot \mathbf{n}_{\ell} & \text{if } \ell \in \mathcal{E}_{\text{bd}}, \end{cases}$$

where we denote the jump of the normal component of  $\mathbf{u}$  across the edge  $\ell$  by  $[\mathbf{u} \cdot \mathbf{n}_{\ell}]$ , and  $\mathbf{n}_{\ell}$  is the outward normal vector.

**2.2.1. Residual estimate.** The first error estimator for lower-order FEM was proposed by Babuška and Rheinboldt [8], and it has become a widely-used estimator in the literature,

$$(2.11) \quad \eta^2 = \sum_{K \in \mathcal{T}_h} h_K^2 \|r_E\|_K^2 + \sum_{\ell \in \mathcal{E}} h_{\ell} \|r_J\|_{\ell}^2.$$

Here  $h_K$  is the diameter of  $K$  and  $h_{\ell}$  is the length of the edge  $\ell$ . It is proved that the estimator is an upper bound for the exact error up to a constant  $C$ ,

$$(2.12) \quad \|u - u_h^k\|_E \leq C\eta,$$

where  $C$  is independent of  $h_K$ . However, the constant  $C$  depends on the shape regularity of the mesh, polynomial degree  $N$ , and the diffusion coefficient  $\kappa(x)$ .

Based on estimator (2.11), Melenk and Wohlmuth developed a residual-based error estimator for  $hp$ -FEM in [25] and proved that the estimator provides an upper bound for the exact error up to a constant,

$$(2.13) \quad \eta^2 = \sum_{K \in \mathcal{T}_h} \frac{h_K^2}{N^2} \|r_E\|_K^2 + \sum_{\ell \in \mathcal{E}} \frac{h_{\ell}}{N} \|r_J\|_{\ell}^2.$$

The constant  $C$  shown in the upper bound (similar to (2.12)) is independent of  $h_K$  and  $N$ , but depends on the shape regularity of the mesh and the diffusion coefficient  $\kappa(x)$ .

In [32, 11, 35], estimator (2.11) is extended to an estimator explicitly depending on  $\kappa(x)$  for linear FEM,

$$(2.14) \quad \eta^2 = \sum_{K \in \mathcal{T}_h} \frac{h_K^2}{\kappa_K} \|r_E\|_K^2 + \sum_{\ell \in \mathcal{E}} \frac{h_\ell}{\kappa_\ell} \|r_J\|_\ell^2.$$

Here  $\kappa_K = \max_{x \in K} \kappa(x)$  and  $\kappa_\ell = \max_{\ell \in \partial K} \kappa_K$ . Assuming  $\kappa(x)$  is quasimonotonically distributed, i.e.  $\kappa(x)$  has at most one local maximum around each node, (2.14) is an upper bound for the exact total error up to a constant depending only on the shape regularity of the mesh for linear element approximation [35]. If this condition does not hold, the constant depends on the bound  $\frac{\max_{x \in \Omega} \kappa(x)}{\min_{x \in \Omega} \kappa(x)}$ .

We combine the  $h$ ,  $N$ , and  $\kappa(x)$  scaling in (2.13) and (2.14) to obtain a heuristic indicator with explicit dependence on these parameters as follows,

$$(2.15) \quad \eta_R = \left( \sum_{K \in \mathcal{T}_h} \eta_{R,K}^2 \right)^{1/2}, \quad \eta_{R,K}^2 = \begin{cases} \frac{h_K^2}{\kappa_K N^2} \|r_E\|_K^2 + \sum_{\ell \in \mathcal{E} \cap \partial K} \frac{h_\ell}{2\kappa_\ell N} \|r_J\|_\ell^2, & \text{if } \ell \in \mathcal{E}_{\text{int}}, \\ \frac{h_K^2}{\kappa_K N^2} \|r_E\|_K^2 + \sum_{\ell \in \mathcal{E} \cap \partial K} \frac{h_\ell}{\kappa_\ell N} \|r_J\|_\ell^2, & \text{if } \ell \in \mathcal{E}_{\text{bd}}. \end{cases}$$

We use  $\eta_{\text{alg}}$  and  $\eta_R$  to approximate  $\|e_{\text{alg}}\|_E$  and  $\|e\|_E$  in (2.7), respectively, and they are included in the following stopping criterion

$$\eta_{\text{alg}} \leq \tau \eta_R.$$

**2.2.2. Modified residual estimate.** We review another explicit estimator proposed for linear elements by Babuška, Durán and Rodríguez in [6, 7]. Let  $\Pi_K h$  be the  $L^2(K)$  projection of the function  $h(x)$  onto a constant for any  $K \in \mathcal{T}_h$ ,

$$\Pi_K h = \frac{1}{|K|} \int_K h \, dx,$$

where  $|K|$  is the area of  $K$ . Further, the projection operator  $\Pi_\ell$  for any edge  $\ell \in \mathcal{E}$  is given by

$$\Pi_\ell g = \frac{1}{|\ell|} \int_\ell g \, ds.$$

Here  $|\ell|$  is the length of the edge  $\ell$ . References [6, 7] provide an estimator for the linear finite element approximation,

$$\eta^2 = \sum_{K \in \mathcal{T}_h} |K|^2 \int_K \frac{(\Pi_K f)^2}{\kappa(x)} dx + \sum_{\ell \in \mathcal{E}} |\ell|^2 \int_\ell \frac{(\Pi_\ell r_J)^2}{\kappa(s)} ds.$$

The estimator is an upper bound for the total error up to a constant depending on  $\kappa(x)$  and the shape regularity of the mesh. For high-order finite elements, as  $\nabla \cdot (\kappa(x) \nabla u_h^k) \neq 0$ , we heuristically generalize the estimator as

$$(2.16) \quad \eta_{\text{MR}} = \left( \sum_{K \in \mathcal{T}_h} |K|^2 \int_K \frac{[\Pi_K (f + \nabla \cdot (\kappa(x) \nabla u_h^k))]^2}{\kappa(x)} dx + \sum_{\ell \in \mathcal{E}} |\ell|^2 \int_\ell \frac{(\Pi_\ell r_J)^2}{\kappa(s)} ds \right)^{1/2}.$$

We use  $\eta_{\text{MR}}$  to approximate  $\|e\|_E$  in (2.7), and the stopping criterion is

$$\eta_{\text{alg}} \leq \tau \eta_{\text{MR}}.$$

*Remark 2.1.* On a regular mesh with isosceles right triangle elements, we have  $\eta_{\text{MR}} \leq \eta_R$  since  $|K| = 4h_K^2$  and  $h_K/\sqrt{2} \leq |\ell| \leq h_K$ . In the case of an anisotropic mesh where  $|K| \ll h_K^2$ , then  $\eta_{\text{MR}} \ll \eta_R$ .

We observe that, given a uniform mesh with mesh size denoted by  $h$ , the scaling of  $\eta_R$  with respect to  $h$  is  $h^{(d-2)/2}$ , whereas the scaling of  $\eta_{\text{MR}}$  is  $h^{d-2}$ , where  $d$  represents the dimension of the space. For two-dimensional space, the mesh size scaling of  $\eta_R$  and  $\eta_{\text{MR}}$  are identical. Nonetheless, these scalings differ when  $d \neq 2$ , which implies  $\eta_{\text{MR}}$  is equivalent to the total error only for  $d = 2$ .

**2.2.3. Flux recovery-based estimator.** Recovery-based a posteriori error estimators have been studied extensively, see [44, 45, 15, 20, 13] for examples. In this work, we use an accuracy enhancing projection to reconstruct the numerical flux and compare it with the original numerical flux  $\kappa(x)\nabla u_h^k$ . In the following, we reconstruct the numerical flux using Brezzi-Douglas-Marini (BDM) elements and solve the local problem element-wise, adopting methods presented in [10, 14]. For the edge  $\ell \in \mathcal{E}$  and  $\ell = \partial K^+ \cap \partial K^-$ , we define the weighted average for  $w$  on  $\ell$

$$\{w\}_\ell^\kappa = \frac{\kappa^-}{\kappa^- + \kappa^+} w^+ + \frac{\kappa^+}{\kappa^- + \kappa^+} w^-,$$

where  $\kappa^-$  and  $\kappa^+$  are the restriction of  $\kappa(x)$  on  $K^-$  and  $K^+$ , respectively. Similarly, we denote the weighted jump for  $w$  on  $\ell$  by

$$[w]_\ell^\kappa = \frac{\kappa^-}{\kappa^- + \kappa^+} (w^+ - w^-).$$

The reconstruction is as follows, fix an element  $K$ , find  $\boldsymbol{\sigma}_K \in (\mathbb{P}_N(K))^2$  satisfying

$$(2.17) \quad \begin{aligned} \int_K \boldsymbol{\sigma}_K \cdot \nabla w &= \int_K \kappa(x) \nabla u_h^k \cdot \nabla w, \quad \forall w \in \mathbb{P}_{N-1}(K), \\ \int_K \boldsymbol{\sigma}_K \cdot \mathbf{S}(\psi) &= \int_K \kappa(x) \nabla u_h^k \cdot \mathbf{S}(\psi), \quad \forall \psi \in M_{N+1}(K), \\ \int_{\ell_i} (\boldsymbol{\sigma}_K \cdot \mathbf{n}) z &= \int_{\ell_i} \{\kappa(x) \nabla u_h^k \cdot \mathbf{n}_{\ell_i}\}_{\ell_i}^\kappa z, \quad \forall z \in \mathbb{P}_N(\ell_i), \ell_i \in \partial K, \quad i = 1, 2, 3. \end{aligned}$$

Here,  $\mathbf{S}(\psi) = (\partial\psi/\partial x_2, -\partial\psi/\partial x_1)$ . Let  $M_N(K)$  be the space of polynomials  $\phi \in \mathbb{P}_N(K)$  vanishing on the boundary of  $K$ ,

$$M_N(K) = \{\phi \in \mathbb{P}_N(K) : \phi|_{\partial K} = 0\}.$$

Let  $\boldsymbol{\rho}_K = \boldsymbol{\sigma}_K - \kappa(x)\nabla u_h^k(x)$ . From (2.17), it satisfies

$$(2.18) \quad \begin{aligned} \int_K \boldsymbol{\rho}_K \cdot \nabla w &= 0, \quad \forall w \in \mathbb{P}_{N-1}(K), \\ \int_K \boldsymbol{\rho}_K \cdot \mathbf{S}(\psi) &= 0, \quad \forall \psi \in M_{N+1}(K), \\ \int_{\ell_i} (\boldsymbol{\rho}_K \cdot \mathbf{n}) z &= \int_{\ell_i} [\kappa(x) \nabla u_h^k \cdot \mathbf{n}_{\ell_i}]_{\ell_i}^\kappa z, \quad \forall z \in \mathbb{P}_N(\ell_i), \ell_i \in \partial K, \quad i = 1, 2, 3. \end{aligned}$$

Now we define the error estimator based on recovery,

$$(2.19) \quad \eta_{\text{BDM}} := \left( \sum_{K \in \mathcal{T}_h} \left\| \kappa(x)^{-1/2} \boldsymbol{\rho}_K \right\|_{\ell_i}^2 \right)^{1/2}.$$

By solving equation (2.18), the jump of the normal component of the numerical flux on the edge  $\ell$ ,  $[\kappa(x) \nabla u_h^k \cdot \mathbf{n}_{\ell_i}]_{\ell_i}^\kappa$ , is lifted to the elementwise function,  $\boldsymbol{\rho}_K$ . We represent the discretized form of the lifting operator by

$$(2.20) \quad \mathbf{y}_K = \mathbf{L}_K \mathbf{d}_K,$$

where  $\mathbf{y}_K$  corresponds to  $\boldsymbol{\rho}_K$ ,  $\mathbf{d}_K$  is associated with  $[\kappa(x) \nabla u_h^k \cdot \mathbf{n}_{\ell_i}]_{\ell_i}^\kappa$ , and  $\mathbf{L}_K$  is the lifting matrix. In each step of the iteration,  $\boldsymbol{\rho}_K$  is obtained by matrix-vector multiplication (2.20) for all elements. However, storing the matrices  $\{\mathbf{L}_K\}$  for all elements can take a significant amount of memory. This demands allocation for  $\mathcal{O}(N^{2d-1})$  entries for each element. In double precision and for  $N = 8$ , it requires 9.5KB per triangle or 232KB per tetrahedron to store the lifting matrix.

To reduce the computational cost and storage, we instead introduce a lower bound for  $\eta_{\text{BDM}}$ . For the element  $K \in \mathcal{T}_h$ ,

$$\|\kappa(x)^{-1/2} \boldsymbol{\rho}_K\|^2 = \mathbf{y}_K^T \mathbf{M}_K \mathbf{y}_K = \mathbf{d}_K^T \mathbf{L}_K^T \mathbf{M}_K \mathbf{L}_K \mathbf{d}_K \geq \mu_K^2 \|\mathbf{d}_K\|^2,$$

where  $\mu_K^2$  is the smallest eigenvalue of  $\mathbf{L}_K^T \mathbf{M}_K \mathbf{L}_K$ , and  $\mathbf{M}_K$  is the mass matrix with elements defined by  $(\mathbf{M}_K)_{ij} = \int_K \kappa(x)^{-1} \phi_j \phi_i dx$ . We define the new error indicator,

$$(2.21) \quad \eta_{\underline{\text{BDM}}} = \left( \sum_{K \in \mathcal{T}_h} \mu_K^2 \|\mathbf{d}_K\|^2 \right)^{1/2}.$$

The error indicator  $\eta_{\underline{\text{BDM}}}$  is a lower bound for  $\eta_{\text{BDM}}$ . Before the first iteration, the linear systems (2.18) are constructed, the eigenvalues  $\mu_K$  are computed and stored, and matrices are discarded. Subsequently, only  $\mu_K$  are used to compute (2.21) in the iterations. Thus, it is less expensive to compute the error indicator (2.21) than (2.19). The stopping criteria for  $\eta_{\text{BDM}}$  and  $\eta_{\underline{\text{BDM}}}$  are

$$\eta_{\text{alg}} \leq \tau \eta_{\text{BDM}}, \quad \eta_{\text{alg}} \leq \tau \eta_{\underline{\text{BDM}}}.$$

However, the second criterion is stricter than the first one due to  $\eta_{\underline{\text{BDM}}}$  being a lower bound for  $\eta_{\text{BDM}}$ .

**3. Stopping Criteria derived from the residual.** In this section, we describe a stopping criterion derived directly from the linear residual and generalize it to Poisson problems with highly variable piecewise constant coefficients.

**3.1. Globally constant coefficient.** The  $n$ -th component of the linear residual  $\mathbf{r}_k = \mathbf{b} - \mathbf{A}\mathbf{x}_k$  is

$$\begin{aligned} (\mathbf{r}_k)_n &= \mathbf{b}_n - (\mathbf{A}\mathbf{x}_k)_n \\ &= (\phi_n, f) - (\phi_n, g)_{\partial\Omega} - \sum_{K \in \mathcal{T}_h} (\kappa(x) \nabla \phi_n, \nabla u_h^k)_K. \end{aligned}$$

Integrating the last term by parts, we obtain

$$\begin{aligned} (\mathbf{r}_k)_n &= \sum_{K \in \mathcal{T}_h} (\phi_n, r_E)_K - \sum_{\ell \in \mathcal{E}} (\phi_n, r_J)_\ell \\ &= (\mathbf{R}_k)_n + (\mathbf{F}_k)_n, \end{aligned}$$

where  $\mathbf{R}_k, \mathbf{F}_k \in \mathbb{R}^{N_s}$ ,  $(\mathbf{R}_k)_n = \sum_{K \in \mathcal{T}_h} (\phi_n, r_E)_K$ , and  $(\mathbf{F}_k)_n = -\sum_{\ell \in \mathcal{E}} (\phi_n, r_J)_\ell$ . We introduce the indicator  $\eta_{\text{RF}}$

$$(3.1) \quad \eta_{\text{RF}} := \|\mathbf{R}_k\| + \|\mathbf{F}_k\|,$$

with the associated stopping criterion:

$$\|\mathbf{r}_k\| \leq \tau \eta_{\text{RF}}.$$

The indicator  $\eta_{\text{RF}}$  is an upper bound for the norm of the residual without any unknown constants involved. Ideally,  $\eta_{\text{RF}}$  should closely track  $\|\mathbf{r}_k\|$  until the total error converges, and the separation between  $\|\mathbf{r}_k\|$  and  $\eta_{\text{RF}}$  should indicate the deviation of the total error from the algebraic error. Furthermore, it is only necessary to compute  $\mathbf{R}_k$ ;  $\mathbf{F}_k = \mathbf{r}_k - \mathbf{R}_k$  can be directly calculated once  $\mathbf{R}_k$  has been determined. Additionally, on a uniform mesh, the  $h$  scaling of  $\eta_{\text{RF}}$  is  $h^{d-2}$ , which is consistent with the scaling of the norm of the residual and  $\eta_{\text{MR}}$ . However, it differs from the  $h$  scaling of the total error except  $d = 2$ .

**3.2. Highly variable piecewise constant coefficient.** We observe that there exists a  $\kappa(x)$  scaling difference between  $\eta_{\text{RF}}$  and the total error. When  $\kappa(x)$  is highly variable, the difference in  $\kappa(x)$  scaling may impact the effectivity of the stopping criterion (3.1). If a good preconditioner is available, leading to a rapid decrease in the CG error, we employ a weighted  $l^2$  norm in (3.1) as an alternative to the standard  $l^2$  norm. This approach ensures that  $\eta_{\text{RF}}$  shares the same  $\kappa(x)$  scaling as the total error. We define a weight vector  $\mathbf{w} \in \mathbb{R}^{N_s}$ ,

$$\mathbf{w}_n = \min_{x \in \omega_n} \kappa(x)^{-1},$$



where  $\omega_n = \text{supp}(\phi_n)$ . The weight  $\mathbf{w}$  is similar to the  $\kappa(x)$  scaling in (2.15). Let

$$\|\mathbf{x}\|_{\mathbf{w}} = (\mathbf{x}^T \text{diag}(\mathbf{w})\mathbf{x})^{1/2}$$

be the weighted  $l^2$  norm of  $\mathbf{x}$ , where  $\text{diag}(\mathbf{w})$  is a diagonal matrix with diagonal elements given by  $\mathbf{w}$ . We define the indicator  $\eta_{\text{RF}}^{\mathbf{w}}$

$$(3.2) \quad \eta_{\text{RF}}^{\mathbf{w}} := \|\mathbf{R}_k\|_{\mathbf{w}} + \|\mathbf{F}_k\|_{\mathbf{w}},$$

and we substitute (3.1) with:

$$(3.3) \quad \|\mathbf{r}_k\|_{\mathbf{w}} \leq \tau \eta_{\text{RF}}^{\mathbf{w}}.$$

In cases where the good preconditioner is not available and CG converges slowly, we partition the domain  $\Omega$  into several subdomains  $\Omega_p$ ,  $p = 1, \dots, P$  based on the value of  $\kappa(x)$ , and compare  $\|\mathbf{r}_k\|_{\mathbf{w}}$  with  $\eta_{\text{RF}}^{\mathbf{w}}$  restricted to these subdomains. The details of the partition are shown in subsection 4.3.1, and the computations of subdomain indicators are presented in Appendix A. We propose a subdomain-based stopping criterion as an alternative to the criterion (3.3)

$$(3.4) \quad \|\mathbf{r}_k^p\|_{\mathbf{w}} \leq \tau \eta_{\text{RF}}^{\mathbf{w},p}, \quad \forall p = 1, \dots, P.$$

Here  $\eta_{\text{RF}}^{\mathbf{w},p} = \|\mathbf{R}_k^p\|_{\mathbf{w}} + \|\mathbf{F}_k^p\|_{\mathbf{w}}$ , and  $\mathbf{R}_k^p$ ,  $\mathbf{F}_k^p$ ,  $\mathbf{r}_k^p$  are vectors obtained by restricting  $\mathbf{R}_k$ ,  $\mathbf{F}_k$ ,  $\mathbf{r}_k$  to subdomain  $\Omega_p$ .

In contrast to criterion (3.3), the subdomain-based criterion (3.4) leads to termination when the weighted norm of the local linear residual is dominated by the local indicator in all subdomains. Although the global total error may have converged, additional iterations may be required for the local errors to converge. As a result, the subdomain-based criterion (3.4) may recommend stopping the iteration slightly later than the criterion (3.3) suggests.

**4. Numerical experiments.** In this section, we test the effectiveness and robustness of stopping criteria with respect to the polynomial degree  $N$ , the shape regularity of the mesh, the diffusion coefficient  $\kappa(x)$ , and the singularity of the solution. We consider four examples. In subsection 4.1, we apply criteria to the Poisson problem with a constant diffusion coefficient and a geometrically regular mesh, demonstrating the validity of the criteria. In subsection 4.2, we use the diamond-shaped mesh, an anisotropic mesh presented in [7], to show the sensitivity of criteria to the shape regularity of the mesh. In subsection 4.3, we demonstrate the performance of criteria for problems with highly variable piecewise constant coefficients and a solution with singularities caused by jumps in the coefficient and the reentrant corner of the L-shape domain, similar to those presented in [2, section 4.1], [17, example 7.5], and [34, section 7.6]. In subsection 4.4, we consider the same problem as described in Example 4.3.2 and solve the linear system using the preconditioned recycling CG, to show that deflation using the recycle subspace is beneficial in achieving efficient termination of the iteration process. We summarize the tested stopping criteria as follows:

- (C1)  $\eta_{\text{alg}} \leq \tau \eta_{\text{R}}$ , where  $\eta_{\text{R}}$  (2.15) is the most commonly used a posteriori error estimator;
- (C2)  $\eta_{\text{alg}} \leq \tau \eta_{\text{MR}}$ , where  $\eta_{\text{MR}}$  (2.16) is an alternative a posteriori error estimator;
- (C3)  $\eta_{\text{alg}} \leq \tau \eta_{\text{BDM}}$ , where  $\eta_{\text{BDM}}$  (2.19) is the error estimator based on flux reconstruction;
- (C4)  $\eta_{\text{alg}} \leq \tau \eta_{\text{BDM}}$ , where  $\eta_{\text{BDM}}$  (2.21) is the lower bound for  $\eta_{\text{BDM}}$ ;
- (C5)  $\|\mathbf{r}_k\|_{\mathbf{w}} \leq \tau \eta_{\text{RF}}^{\mathbf{w}}$ , where  $\eta_{\text{RF}}^{\mathbf{w}}$  (3.2) is an upper bound for  $\|\mathbf{r}_k\|_{\mathbf{w}}$ ;
- (C6)  $\|\mathbf{r}_k^p\|_{\mathbf{w}} \leq \tau \eta_{\text{RF}}^{\mathbf{w},p}$ , for all  $p = 1, \dots, P$ , where  $\eta_{\text{RF}}^{\mathbf{w},p}$  is the subdomain indicator.
- (C7)  $\|\mathbf{r}_k\| \leq \text{TOL} \|\mathbf{r}_0\|$ , where TOL is a preset relative tolerance.

In criteria (C1)-(C3), we compare a posteriori error estimates  $\eta_{\text{R}}$ ,  $\eta_{\text{MR}}$  and  $\eta_{\text{BDM}}$  to the estimate of the algebraic error  $\eta_{\text{alg}}$  (2.8). Moreover, although  $\eta_{\text{BDM}}$  is a lower bound for the estimate  $\eta_{\text{BDM}}$ , we also compare it to  $\eta_{\text{alg}}$  in (C4). Conversely, in criterion (C5), the error indicator  $\eta_{\text{RF}}^{\mathbf{w}}$ , derived from the linear residual, shares greater similarity with the weighted norm of the linear residual, and as a result, it is comparable to the weighted norm of the residual rather than the estimate of the algebraic error. Criterion (C6) is the subdomain-based criterion for problems with highly variable piecewise constant coefficients. Lastly, criterion (C7) is an often used criterion based on the relative residual norm.

We define the quality ratio of a criterion as

$$(4.1) \quad \text{quality ratio} := \frac{\|u - u_h^{k^*}\|_E}{\|u - u_h\|_E},$$

where  $u_h^{k^*}$  is the first solution that satisfies the stopping condition during the iterative process. We note that the quality ratio is always greater than one. If the quality ratio is much greater than one, it implies a premature termination. It is important to note that the quality ratio, which measures the reliability of a stopping criterion, should not be confused with the effectivity index, a common term used in many a posteriori error estimate papers, which indicates the efficiency of an error estimator.

In the following subsections, experiments are performed in Matlab R2019b. When no additional details are provided, we apply the preconditioned conjugate gradient algorithm in [2] with a zero initial guess to solve the linear systems. We use the incomplete Cholesky decomposition preconditioner with empirically selected drop tolerance of  $10^{-4}$  and diagonal shift of  $\alpha = 0.1$ . We choose the delay parameter  $d = 10$  in the algebraic error estimator (2.8). In the subsequent examples, we compare the approximate solution from CG to the linear system (2.5) to the solution obtained using the backslash command in MATLAB. In the tables presented below, we collect the numbers of iterations and quality ratios when applying stopping criteria. For criteria relying on  $\eta_{\text{alg}}$ , the iterations attributed to the delay in the computation of  $\eta_{\text{alg}}$  are not included in the iteration count. However, in practice, all criteria that depend on  $\eta_{\text{alg}}$  require  $d$  additional iterations. In the following figures, all error estimators and indicators are denoted by markers, while all exact errors and the norm of the linear residual are represented without markers.

**4.1. Test problem 1: isotropic mesh.** We consider the Poisson problem (2.1) on  $\Omega = [0, 1]^2$  with the homogeneous Neumann boundary condition,  $\kappa(x) = 1$ , and choose the right-hand side function  $f$  such that the solution to the continuous problem is given by

$$u(x, y) = (1 - x^2)^2(1 - y^2)^2 e^{x+y}.$$

We discretize the problem on a shape regular mesh with 128 isosceles right triangle elements, using piecewise polynomials with degree  $N = 4, 6, 8$ . Since  $\kappa(x) = 1$ , the weight vector  $\mathbf{w}_n = 1, n = 1, \dots, N_s$ . The weighted  $l^2$  norm is the same as the  $l^2$  norm, and  $\eta_{\text{RF}}$  is the same as  $\eta_{\text{RF}}^{\mathbf{w}}$ .

Figure 1 shows the energy norm of the error and the error estimates in the iteration process with  $N = 6$ . We observe that  $\eta_{\text{alg}}$  tracks the  $\mathbf{A}$ -norm error accurately as CG converges fast. Indicators  $\eta_{\text{R}}$ ,  $\eta_{\text{MR}}$ , and  $\eta_{\text{RF}}$  slightly overestimate the total error by a factor less than 10. The estimator  $\eta_{\text{BDM}}$  provides a very tight estimate for the total error. As a lower bound for  $\eta_{\text{BDM}}$ , the indicator  $\eta_{\text{BDM}}$  gives a lower bound for the total error (although not always).

In criteria (C1)-(C5), the parameter  $\tau$  plays a crucial role in determining when to stop the iteration. A small  $\tau$  may result in early termination, while a large  $\tau$  could cause unnecessary iterations. To select a reasonable  $\tau$ , we plot the quality ratio of stopping criteria in Figure 2, varying  $\tau$  from  $1/30$  to  $1/3$ . We find that  $\tau = 1/20$  is an appropriate choice, as all quality ratios remain below 1.1. In subsequent examples, we set  $\tau = 1/20$ .

In Table 1, we present the number of iterations and the corresponding quality ratios (4.1) for  $N = 4, 6, 8$ . We note first that the performances of  $\eta_{\text{R}}$ ,  $\eta_{\text{MR}}$ , and  $\eta_{\text{RF}}$  are very similar due to the regularity of the mesh. They all achieve approximately the same level of accuracy with roughly the same number of iterations. Criteria  $\eta_{\text{BDM}}$  and  $\eta_{\text{BDM}}$  also provide a favorable termination. For empirical criteria based on the relative residual norm, more than 10 additional iterations are required when  $N = 4$ . Moreover, the criterion that requires relative residual norm to be less than  $10^{-6}$  results in premature termination for  $N = 8$ , as the total error has not yet sufficiently converged at the stopping point. Overall, the first five criteria provide reliable and efficient alternatives for this problem.

**4.2. Test problem 2: highly anisotropic mesh.** To demonstrate the robustness of stopping criteria with respect to the shape regularity of the mesh, we solve the PDE with the same solution, diffusion coefficient  $\kappa(x)$ , right-hand side function  $f$ , and boundary condition as subsection 4.1, but on a highly anisotropic mesh with 64 triangle elements. Figure 3 shows the

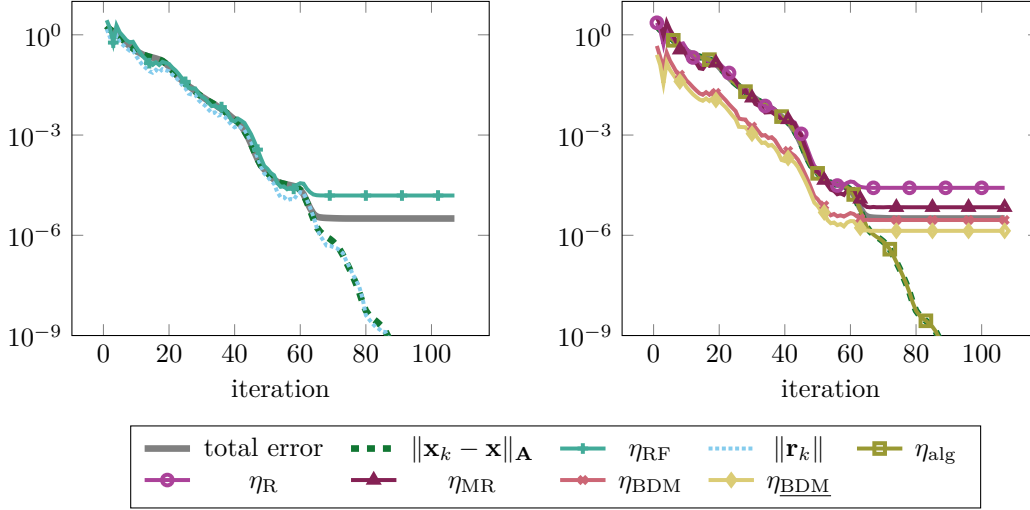


Fig. 1: Convergence history for test problem 1 (isotropic mesh) with  $N = 6$ . Left: the total error, the  $\mathbf{A}$ -norm error  $\|\mathbf{x}_k - \mathbf{x}\|_{\mathbf{A}}$ , the norm of the linear residual  $\|\mathbf{r}_k\|$  and  $\eta_{\text{RF}}$ . Right: the total error, the  $\mathbf{A}$ -norm error  $\|\mathbf{x}_k - \mathbf{x}\|_{\mathbf{A}}$  and its estimator  $\eta_{\text{alg}}$  (delay parameter  $d = 10$ ), and the error indicators  $\eta_{\text{R}}$ ,  $\eta_{\text{MR}}$ ,  $\eta_{\text{BDM}}$  and  $\eta_{\text{BDM}}$ .

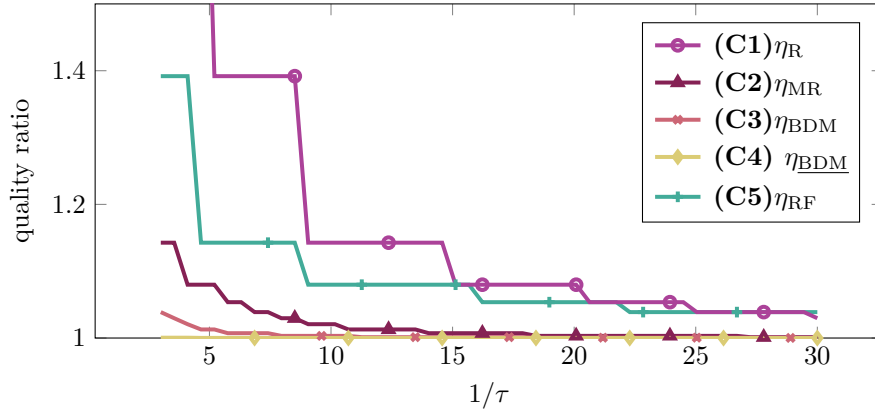


Fig. 2: Sensitivity of the stopping criteria quality ratios with respect to  $\tau$  for test problem 1.

Table 1: Numbers of iterations (iter) and quality ratios (qual. (4.1)) resulting from applying stopping criteria to the solution of test problem 1.

Criterion	$N = 4$		$N = 6$		$N = 8$	
	iter	qual.	iter	qual.	iter	qual.
$\eta_{\text{alg}} \leq \tau \eta_{\text{R}}$	28	1.02	66	1.08	128	1.13
$\eta_{\text{alg}} \leq \tau \eta_{\text{MR}}$	28	1.02	73	1.00	136	1.00
$\eta_{\text{alg}} \leq \tau \eta_{\text{BDM}}$	35	1.00	75	1.00	138	1.00
$\eta_{\text{alg}} \leq \tau \eta_{\text{BDM}}$	36	1.00	76	1.00	141	1.00
$\ \mathbf{r}_k\  \leq \tau \eta_{\text{RF}}$	28	1.02	67	1.05	130	1.04
$\ \mathbf{r}_k\  \leq 10^{-6} \ \mathbf{r}_0\ $	43	1.00	68	1.04	102	388.80
$\ \mathbf{r}_k\  \leq 10^{-8} \ \mathbf{r}_0\ $	52	1.00	80	1.00	120	3.32
$\ \mathbf{r}_k\  \leq 10^{-10} \ \mathbf{r}_0\ $	59	1.00	95	1.00	139	1.00

diamond-shaped mesh used in [7]. We employ a mesh containing triangles with an aspect ratio

$r = 1/32$ , and the minimal angle is approximately  $\alpha = \arctan(r) \approx \frac{\pi}{50}$ .

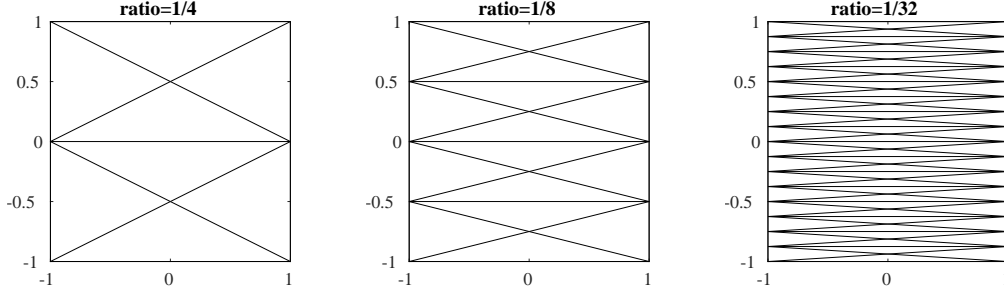


Fig. 3: Diamond-shaped anisotropic mesh with ratio  $1/4$ ,  $1/8$ ,  $1/32$ . We use the mesh with ratio  $1/32$  in test problem 2.

Table 2 presents the performance of stopping criteria with  $N = 4, 6, 8$ . Due to the highly anisotropic mesh, the first criterion  $\eta_{\text{alg}} \leq \tau\eta_{\text{R}}$  appears to lose reliability when  $N = 8$ . Recall that the mesh size  $h$  scaling in element residual of  $\eta_{\text{R}}$  is  $h_K^2$ , where  $h_K$  is the diameter of the element  $K$ , while the  $h$  scaling in  $\eta_{\text{MR}}$  and  $\eta_{\text{RF}}$  are  $|K|$ . The area  $|K|$  is much less than  $h_K^2$  for anisotropic elements. As a result,  $\eta_{\text{R}}$  overestimates the total error and thus the criterion  $\eta_{\text{alg}} \leq \tau\eta_{\text{R}}$  suggests stopping prematurely. In contrast,  $\eta_{\text{MR}}$  demonstrates good performance due to the correct  $h$  scaling. The performance of  $\eta_{\text{alg}} \leq \tau\eta_{\text{BDM}}$  offers the reliable termination, and the criterion  $\eta_{\text{alg}} \leq \tau\eta_{\text{BDM}}$  leads to slightly late termination. As for the results in subsection 4.1, the criterion  $\|\mathbf{r}_k\| \leq \tau\eta_{\text{RF}}$  provides an accurate estimate for the termination. Furthermore, criteria based on the relative residual norm no longer result in early termination as the discretization error is greater than that for subsection 4.1, due to the small angles and fewer elements in the anisotropic mesh. However, the criteria based on the relative residual norm require at least 50 additional iterations.

Table 2: Numbers of iterations (iter) and quality ratios (qual. (4.1)) resulting from applying stopping criteria to the solution of test problem 2 with the diamond-shaped anisotropic mesh.

Criterion	$N = 4$		$N = 6$		$N = 8$	
	iter	qual.	iter	qual.	iter	qual.
$\eta_{\text{alg}} \leq \tau\eta_{\text{R}}$	7	1.60	49	1.84	141	4.78
$\eta_{\text{alg}} \leq \tau\eta_{\text{MR}}$	26	1.01	78	1.02	187	1.03
$\eta_{\text{alg}} \leq \tau\eta_{\text{BDM}}$	31	1.00	91	1.00	198	1.00
$\eta_{\text{alg}} \leq \tau\eta_{\text{BDM}}$	49	1.00	112	1.00	209	1.00
$\ \mathbf{r}_k\  \leq \tau\eta_{\text{RF}}$	28	1.00	88	1.01	199	1.00
$\ \mathbf{r}_k\  \leq 10^{-6}\ \mathbf{r}_0\ $	87	1.00	155	1.00	235	1.00
$\ \mathbf{r}_k\  \leq 10^{-8}\ \mathbf{r}_0\ $	96	1.00	173	1.00	268	1.00
$\ \mathbf{r}_k\  \leq 10^{-10}\ \mathbf{r}_0\ $	105	1.00	189	1.00	296	1.00

The results in Table 2 are also illustrated in Figure 4. As for subsection 4.1,  $\eta_{\text{alg}}$  closely follows the  $\mathbf{A}$ -norm of the algebraic error. The estimator  $\eta_{\text{R}}$  overestimates the energy norm by a constant of more than 20 due to the the highly anisotropic mesh. Both  $\eta_{\text{MR}}$  and  $\eta_{\text{RF}}$  are roughly four times greater than the exact total error. This discrepancy can be compensated by adjusting the parameter  $\tau = 1/20$ . Meanwhile,  $\eta_{\text{BDM}}$  gives a tight estimate for the total error, as for subsection 4.1, and  $\eta_{\text{BDM}}$  underestimates the total error. Overall, we find criteria  $\eta_{\text{MR}}$ ,  $\eta_{\text{BDM}}$  and  $\eta_{\text{RF}}$  perform reasonably well in this example. However,  $\eta_{\text{R}}$  overestimates the error by a relatively large factor, resulting in early termination. Conversely,  $\eta_{\text{BDM}}$  underestimates the total error, leading to a number of additional iterations. All criteria depending on a fixed relative residual norm require a large number of iterations.

**4.3. Test problem 3: highly variable piecewise constant coefficients.** In order to demonstrate the effectiveness of the stopping criteria with variable diffusion coefficient  $\kappa(x)$ , we

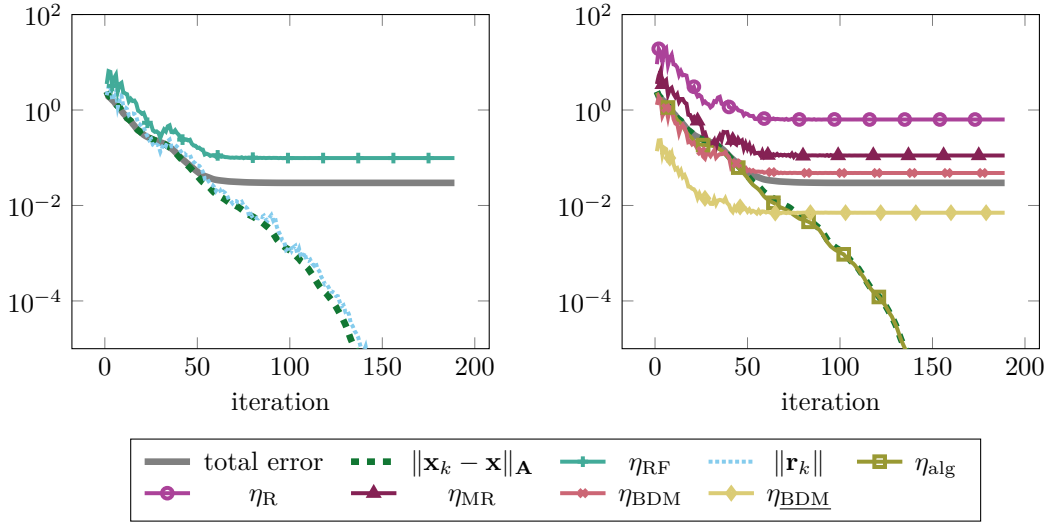


Fig. 4: Convergence history for the diamond-shaped anisotropic mesh in test problem 2 with  $N = 6$ . Left: the total error, the  $\mathbf{A}$ -norm error  $\|\mathbf{x}_k - \mathbf{x}\|_{\mathbf{A}}$ , the norm of the linear residual  $\|\mathbf{r}_k\|$  and  $\eta_{\text{RF}}$ . Right: the total error, the  $\mathbf{A}$ -norm error  $\|\mathbf{x}_k - \mathbf{x}\|_{\mathbf{A}}$  and its estimator  $\eta_{\text{alg}}$ , and the error indicators  $\eta_{\text{R}}, \eta_{\text{MR}}, \eta_{\text{BDM}}, \eta_{\text{BDM}}$ .

consider two problems on a L-shape domain with highly variable piecewise constant coefficients and the homogeneous Dirichlet boundary condition, similar to the example considered in [2, Section 4.1]. As shown in Figure 5, the domain  $\Omega$  is partitioned into four subdomains, and  $\kappa(x)$  is constant on each subdomain.

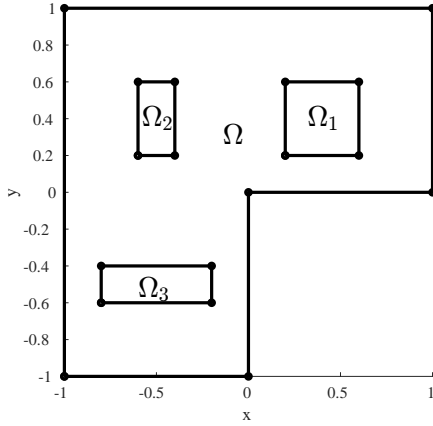


Fig. 5: Geometry of the domain  $\Omega$  in test problem 3.

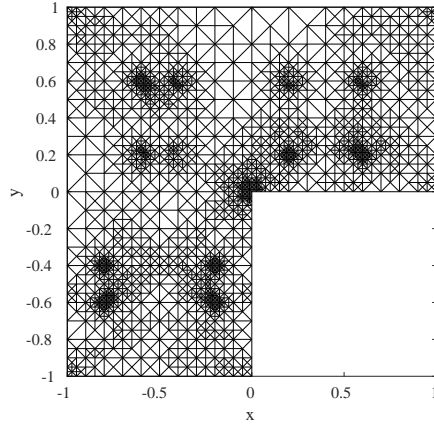


Fig. 6: Mesh with 3733 elements for Example 4.3.1 in test problem 3.

EXAMPLE 4.3.1. We choose  $f_1(x) = 0.1$ , and

$$\kappa_1(x) = \begin{cases} 1, & x \in \Omega \setminus \{\Omega_1 \cup \Omega_2 \cup \Omega_3\} \\ 10^{-6}, & x \in \Omega_1 \cup \Omega_2 \cup \Omega_3. \end{cases}$$

EXAMPLE 4.3.2. We have  $f_2(x) = 10$ , and

$$\kappa_2(x) = \begin{cases} 1, & x \in \Omega \setminus \{\Omega_1 \cup \Omega_2 \cup \Omega_3\} \\ 10^6, & x \in \Omega_1 \cup \Omega_2 \cup \Omega_3. \end{cases}$$

We begin with a structured mesh of  $\Omega$  consisting of 150 isosceles right triangle elements, and refine the mesh adaptively, using  $\eta_{R,K}$  (2.15) as an error indicator. The adaptive mesh refinement strategy is to refine all elements where  $\eta_{R,K}$  is greater than the average  $\eta_{R,K}$ . The mesh, as illustrated in Figure 6, consists of 3733 elements and is used in Example 4.3.1. The refinement is concentrated near corners of  $\Omega_1$ ,  $\Omega_2$ ,  $\Omega_3$  and the reentrant corner of the L-shape domain. We assume that the solution obtained from a mesh refined six times is an accurate approximation to the exact solution of the continuous problem for Example 4.3.1. In this example, we do not examine  $\eta_{MR}$  as the mesh is regular and the performance of  $\eta_{MR}$  is similar to  $\eta_R$ .

Table 3: Numbers of iterations (iter) and quality ratios (qual. (4.1)) resulting from applying stopping criteria to the solution in test problem 3 with the highly variable coefficient.

$\kappa(x), f(x)$	Criterion	$N = 4$		$N = 6$		$N = 8$	
		iter	qual.	iter	qual.	iter	qual.
$\kappa_1(x), f_1(x)$	$\eta_{\text{alg}} \leq \tau \eta_R$	76	1.03	139	1.07	212	1.11
	$\eta_{\text{alg}} \leq \tau \eta_{\text{BDM}}$	86	1.00	155	1.00	243	1.01
	$\eta_{\text{alg}} \leq \tau \eta_{\text{BDM}}^{\mathbf{w}}$	91	1.00	172	1.00	264	1.00
	$\ \mathbf{r}_k\ _{\mathbf{w}} \leq \tau \eta_{\text{RF}}^{\mathbf{w}}$	70	1.13	131	1.14	201	1.26
	$\ \mathbf{r}_k\  \leq 10^{-8} \ \mathbf{r}_0\ $	192	1.00	334	1.00	506	1.00
$\kappa_2(x), f_2(x)$	$\eta_{\text{alg}} \leq \tau \eta_R$	244	32.95	419	53.17	631	93.99
	$\eta_{\text{alg}} \leq \tau \eta_{\text{BDM}}$	252	32.95	435	53.17	663	93.99
	$\eta_{\text{alg}} \leq \tau \eta_{\text{BDM}}^{\mathbf{w}}$	376	2.46	652	3.78	981	7.79
	$\ \mathbf{r}_k\ _{\mathbf{w}} \leq \tau \eta_{\text{RF}}^{\mathbf{w}}$	241	32.95	417	53.17	632	93.99
	$\ \mathbf{r}_k\  \leq 10^{-8} \ \mathbf{r}_0\ $	634	1.00	1104	1.00	1654	1.00

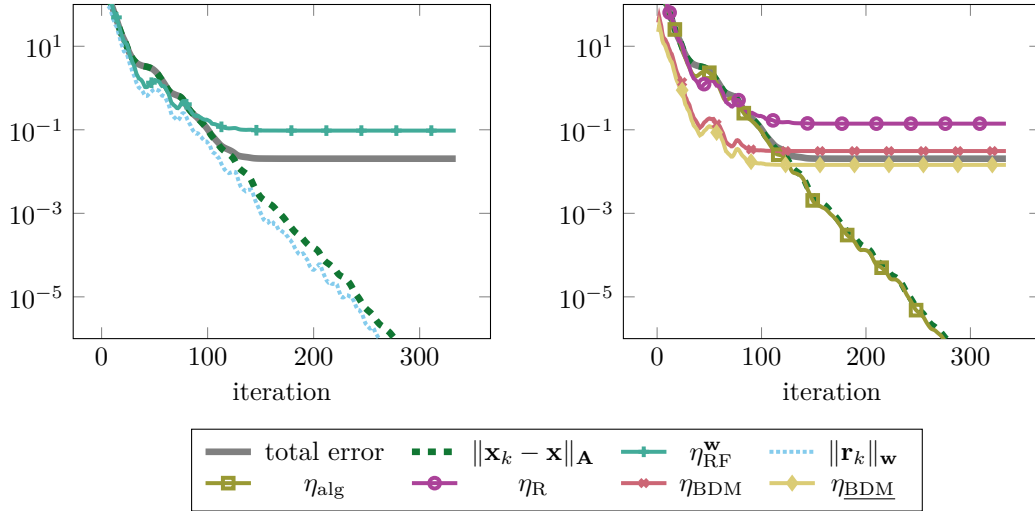


Fig. 7: Convergence history of the Poisson problem with  $f_1(x)$  and a highly variable coefficient  $\kappa_1(x)$  in Example 4.3.1 and polynomial degree  $N = 6$ . Left: the total error, the  $\mathbf{A}$ -norm error  $\|\mathbf{x}_k - \mathbf{x}\|_{\mathbf{A}}$ , the weighted norm of the linear residual  $\|\mathbf{r}_k\|_{\mathbf{w}}$  and  $\eta_{\text{RF}}^{\mathbf{w}}$ . Right: the total error, the  $\mathbf{A}$ -norm error  $\|\mathbf{x}_k - \mathbf{x}\|_{\mathbf{A}}$  and its estimator  $\eta_{\text{alg}}$  (delay parameter  $d = 10$ ), and error estimators  $\eta_R$  and  $\eta_{\text{BDM}}$ .

Figure 7 exhibits the convergence history of the energy norm of the error and its error estimates in the whole domain  $\Omega$  for Example 4.3.1 with  $N = 6$ . The total error converges rapidly, and the norm of the residual decreases roughly monotonically. We note that the algebraic estimator  $\eta_{\text{alg}}$  provides an accurate approximation to the  $\mathbf{A}$ -norm of the algebraic error. The left part of Figure 7 demonstrates that the separation of  $\eta_{\text{RF}}^{\mathbf{w}}$  and  $\|\mathbf{r}_k\|_{\mathbf{w}}$  is close to the separation of the total error and the algebraic error, halting the iteration at a reasonable point. On the right

part of Figure 7, the estimator  $\eta_R$  slightly overestimates the total error. The indicators  $\eta_{BDM}$  and  $\eta_{BDM}$  follow the total error closely.

Table 3 displays the results for Example 4.3.1 with  $N = 4, 6, 8$ . The criterion  $\eta_{alg} \leq \tau\eta_R$  exhibits satisfactory performance. As for results of subsection 4.1 and subsection 4.2, applying  $\eta_{alg} \leq \tau\eta_{BDM}$  demonstrates a favorable termination, while the criterion  $\eta_{alg} \leq \tau\eta_{BDM}$  leads to slightly delayed termination. The criterion  $\|\mathbf{r}_k\|_{\mathbf{w}} \leq \tau\eta_{RF}^{\mathbf{w}}$  yields a small quality ratio and requires a small number of iterations. Similarly, although the empirical criterion  $\|\mathbf{r}_k\| \leq 10^{-8}\|\mathbf{r}_0\|$  achieves a quality ratio 1, it requires a larger number of additional iterations, compared with other criteria.

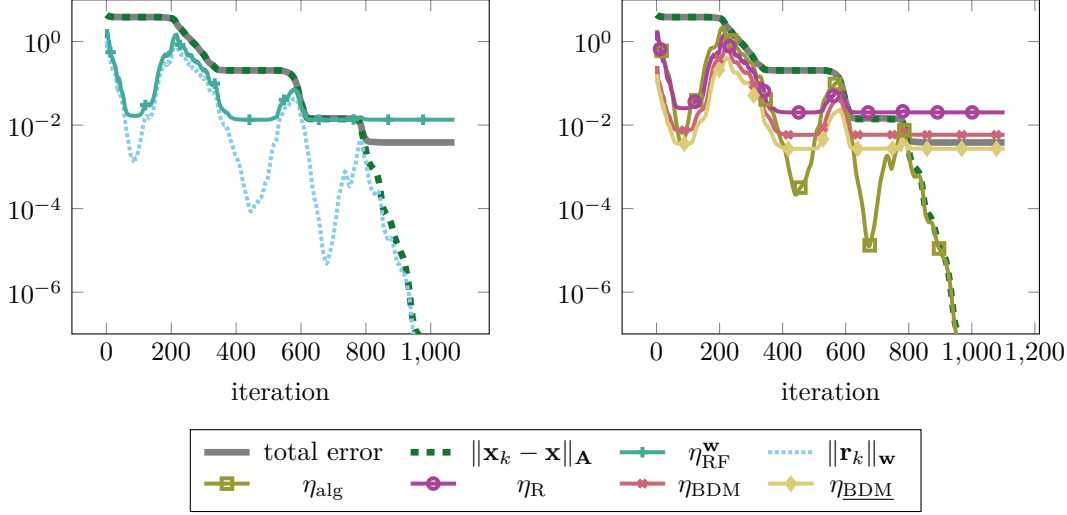


Fig. 8: Convergence history of the Poisson problem with  $f_2(x)$  and a highly variable coefficient  $\kappa_2(x)$  in Example 4.3.2 and polynomial degree  $N = 6$ . Left: the total error, the  $\mathbf{A}$ -norm error  $\|\mathbf{x}_k - \mathbf{x}\|_{\mathbf{A}}$ , the weighted norm of the linear residual  $\|\mathbf{r}_k\|_{\mathbf{w}}$  and  $\eta_{RF}^{\mathbf{w}}$ . Right: the total error, the  $\mathbf{A}$ -norm error  $\|\mathbf{x}_k - \mathbf{x}\|_{\mathbf{A}}$  and its estimator  $\eta_{alg}$  (delay parameter  $d = 10$ ), and error indicators  $\eta_R$  and  $\eta_{BDM}$ .

Example 4.3.2 is more challenging than Example 4.3.1. Analysis for similar problems in one dimensional space is provided in [41]. We refine the mesh such that the mesh consists of 5747 elements in solving Example 4.3.2. Figure 8 depicts the convergence history of the energy norm of errors and their estimates. The energy norm of the total error and the  $\mathbf{A}$ -norm of the algebraic error display several plateaus in the iteration process. Moreover, the norm of the residual is highly oscillatory when the total error is in the first three plateaus. All error estimators and indicators follow the trend of the residual, rather than the trend of the total error since all indicators are based on local residuals and jump residuals. In particular, the right part of Figure 8 shows that with the delay parameter  $d = 10$ ,  $\eta_{alg}$  does not provide an accurate approximation of the exact algebraic error. As also highlighted in [2, Section 4.1], a large value of  $d$  is necessary to obtain an accurate algebraic error estimator. In this example, the estimator  $\eta_{alg}$  with  $d$  exceeding 150, may serve as an effective estimator. However, it requires an extra 150 iterations to obtain the estimator. Since  $\eta_{alg}$  substantially underestimates the algebraic error at several phases of the iteration, its inferior performance contributes to the failure of criteria  $\eta_{alg} \leq \tau\eta_R$ ,  $\eta_{alg} \leq \tau\eta_{BDM}$ , and  $\eta_{alg} \leq \tau\eta_{BDM}$ .

The results for Example 4.3.2 are also presented in Table 3. The criteria based on  $\eta_R$ ,  $\eta_{BDM}$ , and  $\eta_{RF}^{\mathbf{w}}$  result in early termination with the same quality ratios, as they all suggests stopping at the second plateau (approximately from 400 to 600 steps). The termination resulting from the criterion  $\eta_{alg} \leq \tau\eta_{BDM}$  is slightly early, since the iteration stops at the third plateau. As expected, the criterion based on the relative norm of the residual requires a large number of iterations.

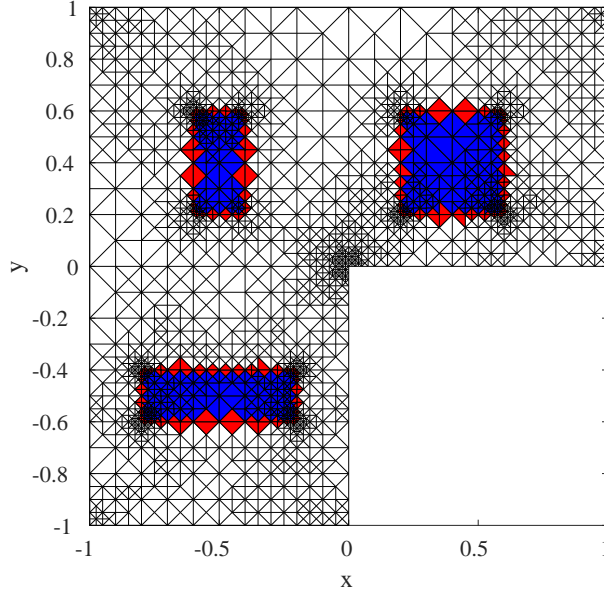


Fig. 9: Partition of  $\Omega$  in test problem 3: interior subdomain (blue), overlap subdomain (red) and exterior subdomain (white).

**4.3.1. Subdomain-based stopping criterion.** To address the suboptimal performance of  $\eta_{\text{RF}}^{\mathbf{w}}$  for problems with a highly variable coefficient in Example 4.3.2, we consider the subdomain-based stopping criterion in (3.4). As illustrated in Figure 9, we partition the domain  $\Omega$  into three subdomains: the interior subdomain colored in blue, the overlap subdomain colored in red and the exterior subdomain in white. Table 4 demonstrates that quality ratios of applying the subdomain-based stopping criterion are one. Compared with the results from Table 3, the subdomain-based stopping criterion results in late termination for Example 4.3.1. For Example 4.3.2, it is the only criterion, in addition to the criterion based on relative residual norm, that leads to reasonable termination. Moreover, the subdomain-based stopping criterion requires fewer iterations than the relative residual norm criterion. It strikes a balance between efficiency and reliability, thereby making it a competitive choice. The computation of the subdomain-based stopping criterion is presented in Appendix A.

Table 4: Numbers of iterations (iter) and quality ratios (qual. (4.1)) resulting from applying the subdomain-based stopping criterion to the solution in Example 4.3.1 and Example 4.3.2.

$\kappa(x), f(x)$	Criterion	$N = 4$		$N = 6$		$N = 8$	
		iter	qual.	iter	qual.	iter	qual.
$\kappa_1(x), f_1(x)$	$\ \mathbf{r}_k^p\ _{\mathbf{w}} \leq \tau \eta_{\text{RF}}^{\mathbf{w},p}, \forall p$	79	1.02	196	1.00	399	1.00
$\kappa_2(x), f_2(x)$	$\ \mathbf{r}_k^p\ _{\mathbf{w}} \leq \tau \eta_{\text{RF}}^{\mathbf{w},p}, \forall p$	551	1.00	997	1.00	1505	1.00

Figure 10 (b), (c), and (d) display the convergence history of the error indicators within subdomains for Example 4.3.2. In comparison to the convergence in the interior domain,  $\eta_{\text{RF}}^{\mathbf{w},p}$  in the overlap and exterior subdomains deviate from  $\|\mathbf{r}_k^p\|_{\mathbf{w}}$  much earlier. The early separation of the weighted norm of the residual  $\|\mathbf{r}_k^p\|_{\mathbf{w}}$  and the indicator  $\eta_{\text{RF}}^{\mathbf{w},p}$  in the exterior subdomain leading to the early termination in the whole domain, since the indicator  $\eta_{\text{RF}}^{\mathbf{w},p}$  in the exterior subdomain is dominant in the total  $\eta_{\text{RF}}^{\mathbf{w}}$ . However, the local indicator  $\eta_{\text{RF}}^{\mathbf{w},p}$  in the interior subdomain diverges from the local residual  $\|\mathbf{r}_k^p\|_{\mathbf{w}}$  at around the iteration 950. The subdomain-based stopping criterion ensures that the iteration terminates when the local indicator  $\eta_{\text{RF}}^{\mathbf{w},p}$  in the interior subdomain tends to stagnate. In solving the Poisson problem Example 4.3.2, the subdomain stopping criterion is more conservative and more reliable in practice. Similarly, the partition can be generalized to the other criteria based on error estimators.



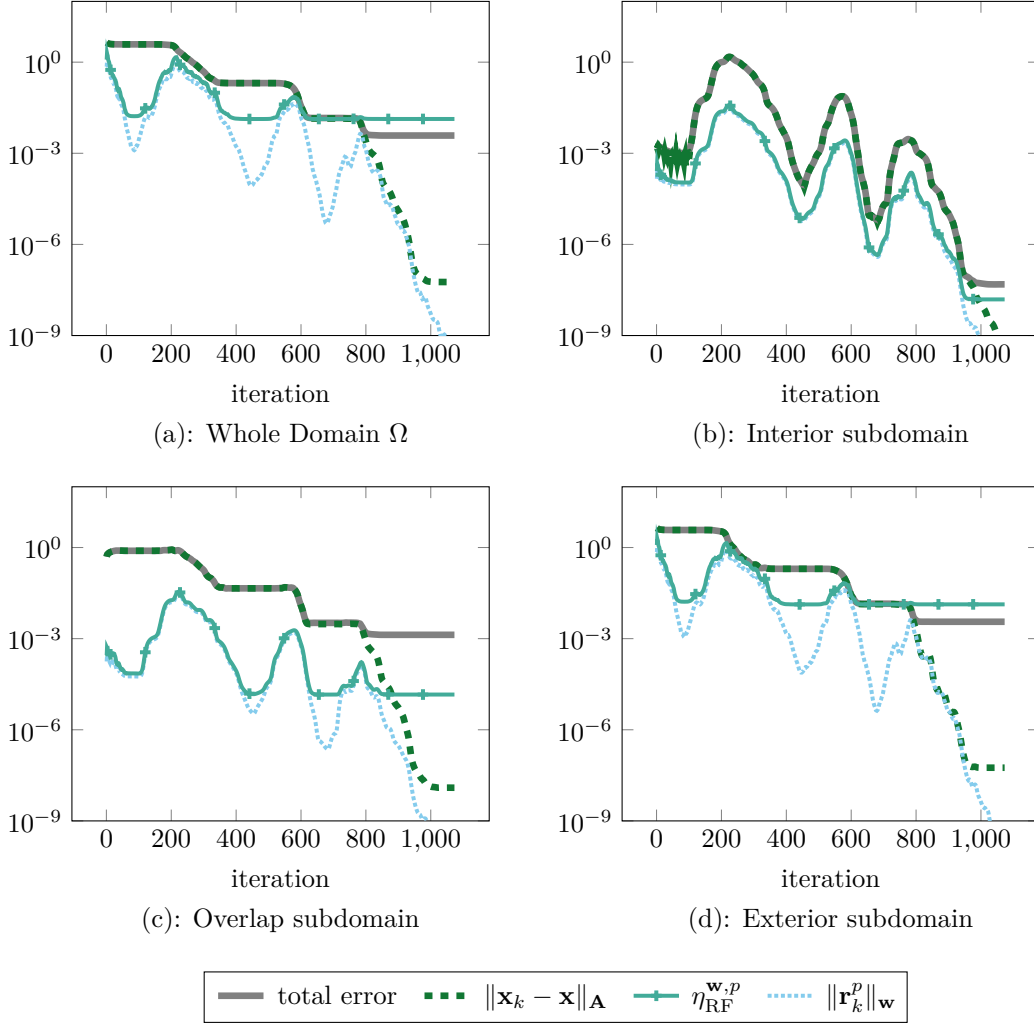


Fig. 10: Convergence history of the Poisson problem with a highly variable coefficient,  $\kappa_2(x)$ , in Example 4.3.2 and polynomial degree  $N = 6$ . The total error, the exact  $\mathbf{A}$ -norm error  $\|\mathbf{x}_k - \mathbf{x}\|_{\mathbf{A}}$ , the weighted norm of the subdomain linear residual  $\|\mathbf{r}_k^p\|_{\mathbf{w}}$  and subdomain error indicator  $\eta_{\text{RF}}^{\mathbf{w},p}$ .

**4.4. Test problem 4: revisiting the problem with highly variable coefficients.** The results of Example 4.3.2 exhibit significant oscillations of the residual norm, as the linear system is very ill-conditioned. Although preconditioned CG minimizes  $\|\mathbf{x}_k - \mathbf{x}\|_{\mathbf{A}}$ , the ratio  $\|\mathbf{r}_k\|_2 / \|\mathbf{x}_k - \mathbf{x}\|_{\mathbf{A}}$  can range (in principle) from  $\lambda_{\min}$  to  $\lambda_{\max}$ , which allows for substantial oscillations if the condition number of  $\mathbf{A}$  is large. This effect can be mitigated by better preconditioning and/or deflated versions of CG [37, 31, 18]. Deflation, in particular, can remove the smallest eigenvalues (and largest if desired) and drastically improve the condition number, generally leading to convergence of the residual norm that is monotonic or nearly so. Consequently, deflation and better preconditioning allow for a small delay parameter  $d$  and more reliable behavior of error estimators, improving the efficiency of stopping criteria.

To demonstrate the benefits of deflation in this context, we also run Example 4.3.2, using the recycling conjugate gradients method (recycling CG) [12, 38, 30]. Recycling CG is appropriate for Poisson problems as they often occur in a sequence of linear systems arising as the pressure Poisson solve in incompressible Navier-Stokes problems [1]. In this example, the recycle space is obtained from recycling CG by solving the Poisson equation with the source function  $f = 10 + 50 \sin x$ . The recycle space basis has twenty orthonormal vectors that approximate eigenvectors corresponding to the first twenty smallest eigenvalues of the linear system, and the subspace is

updated every twenty CG iterations.

Table 5: Numbers of iterations (iter.) and quality ratios (qual. (4.1)) of stopping criteria to the solution in Example 4.3.2 solved by the preconditioned recycling CG.

Criterion	$N = 4$		$N = 6$		$N = 8$	
	iter	qual.	iter	qual.	iter	qual.
$\eta_{\text{alg}} \leq \tau \eta_{\text{R}}$	44	1.03	67	1.04	106	1.06
$\eta_{\text{alg}} \leq \tau \eta_{\text{BDM}}$	54	1.00	78	1.00	129	1.00
$\eta_{\text{alg}} \leq \tau \eta_{\text{BDM}}$	60	1.00	86	1.00	139	1.00
$\ \mathbf{r}_k\ _{\mathbf{w}} \leq \tau \eta_{\text{RF}}^{\mathbf{w}}$	43	1.04	66	1.04	107	1.06
$\ \mathbf{r}_k^p\ _{\mathbf{w}} \leq \tau \eta_{\text{RF}}^{\mathbf{w},p}, \forall p$	95	1.00	155	1.00	288	1.00
$\ \mathbf{r}_k\  \leq 10^{-8} \ \mathbf{r}_0\ $	131	1.00	191	1.00	324	1.00

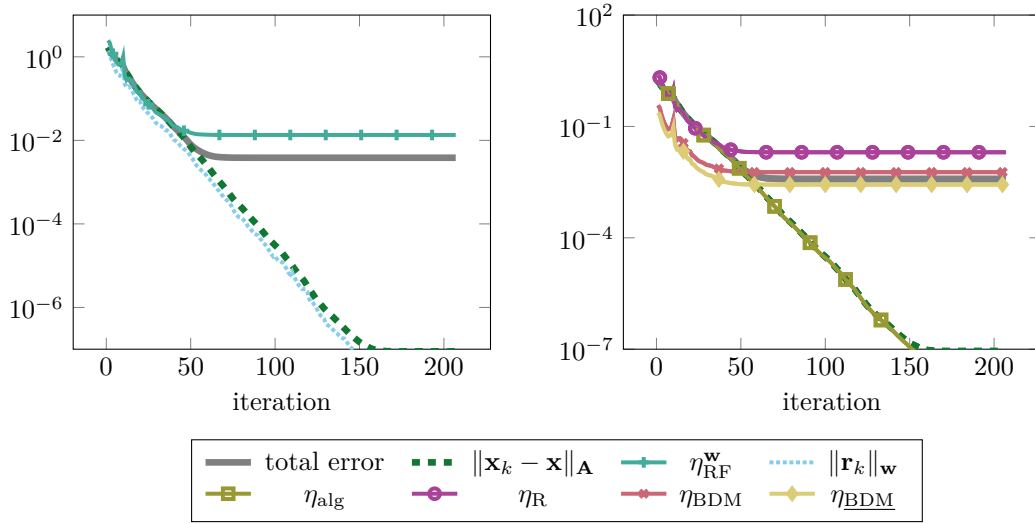


Fig. 11: Convergence history of the Poisson problem with a highly variable diffusion coefficient and a good recycle space in test problem 4, with the polynomial degree  $N = 6$  and the delay parameter  $d = 10$ .

Table 5 displays the number of iterations and quality ratios of criteria. Criteria  $\eta_{\text{R}}$ ,  $\eta_{\text{RF}}^{\mathbf{w}}$ ,  $\eta_{\text{BDM}}$ , and  $\eta_{\text{BDM}}$  have desired quality ratios. The indicator  $\eta_{\text{BDM}}$ , as a lower bound for  $\eta_{\text{BDM}}$ , requires more iterations. The subdomain-based criterion also requires a great number of extra iterations. If the norm of the residual exhibits a roughly monotonic decrease, employing this criterion becomes unnecessary. Consistent with previous examples, the criterion based on relative norm of the residual expends a significant number of unnecessary iterations.

Figure 11 illustrates the history of errors norm and indicators for this problem solved by the preconditioned recycling conjugate gradient algorithm. As the well-chosen recycle subspace lessens the impact of the ill-conditioned linear system and consequently, the residual in the iterative process tends to decrease monotonically. The algebraic error estimator and a posteriori error estimators capture the behavior of exact errors well. The separation between  $\|\mathbf{r}_k\|_{\mathbf{w}}$  and  $\eta_{\text{RF}}^{\mathbf{w}}$  almost coincides with the separation between the algebraic error and the total error. This is the instance where employing suitable recycle subspace can be helpful in the efficient termination of iteration process.

**4.5. Results summary.** We present a summary of the numerical experiments in this section as a score sheet in Table 6. The methods are scored by whether they lead to premature termination with a quality ratio greater than 2 (0 points), whether they suggest stopping slightly

early or slightly late (1 point), or if the quality ratio is less than 1.5 and the iteration stops at roughly the optimal point, ensuring adequate accuracy and fewer iterations (2 points).

We summarize the performance of tested stopping criteria as follows:

- (C1)  $\eta_{\text{alg}} \leq \tau\eta_{\text{R}}$ . The estimator  $\eta_{\text{R}}$  is sensitive to the shape regularity of the mesh, and thus it may result in inaccurate termination for anisotropic meshes.
- (C2)  $\eta_{\text{alg}} \leq \tau\eta_{\text{MR}}$ . This criterion is excluded from the table as  $\eta_{\text{MR}}$  has the same  $h$  scaling as the total error only in two dimensions.
- (C3)  $\eta_{\text{alg}} \leq \tau\eta_{\text{BDM}}$ . The estimator  $\eta_{\text{BDM}}$  provides the most accurate estimate for the total error; however, it is computationally expensive and requires a large amount of memory.
- (C4)  $\eta_{\text{alg}} \leq \tau\eta_{\text{BDM}}$ . While  $\eta_{\text{BDM}}$  is less costly and more reliable than  $\eta_{\text{BDM}}$ , it sometimes leads to extra iterations, as  $\eta_{\text{BDM}}$  is a lower bound for  $\eta_{\text{BDM}}$ .
- (C5)  $\|\mathbf{r}_k\|_{\mathbf{w}} \leq \tau\eta_{\text{RF}}^{\mathbf{w}}$ . This criterion offers a competitive option as long as  $\eta_{\text{RF}}^{\mathbf{w}}$  closely tracks  $\|\mathbf{r}_k\|_{\mathbf{w}}$ , which is usually the case except for Example 4.3.2.
- (C6)  $\|\mathbf{r}_k^p\|_{\mathbf{w}} \leq \tau\eta_{\text{RF}}^{\mathbf{w},p}$ , for all  $p = 1, \dots, P$ . This is the only tested criterion that provides reliable termination for Example 4.3.2.

All criteria depending on the algebraic error estimator  $\eta_{\text{alg}}$  fail when the algebraic error remains almost constant for a relatively large number of iterations. In such cases, with a small delay parameter  $d$ , the estimator  $\eta_{\text{alg}}$  is not accurate, and selecting an appropriate  $d$  can be challenging. Additionally, in practice, the criteria relying on  $\eta_{\text{alg}}$  include an additional  $d$  iterations (with  $d = 10$  in all experiments) required to compute  $\eta_{\text{alg}}$ .

Table 6: Summary of performance of stopping criteria on the numerical examples. If the iteration stops too early, score=0; if the iteration stops slightly late or slightly early, score=1; if it stops close to the optimal point, score=2.

Criterion	Test 1: regular	Test 2: anisotropic	Test 3.1: $\kappa_1, f_1$	Test 3.2: $\kappa_2, f_2$	Test 4: w. defl.	Total score
(C1) $\eta_{\text{alg}} \leq \tau\eta_{\text{R}}$	2	0	2	0	2	6
(C3) $\eta_{\text{alg}} \leq \tau\eta_{\text{BDM}}$	2	2	2	0	2	8
(C4) $\eta_{\text{alg}} \leq \tau\eta_{\text{BDM}}$	2	1	1	0	2	6
(C5) $\ \mathbf{r}_k\ _{\mathbf{w}} \leq \tau\eta_{\text{RF}}^{\mathbf{w}}$	2	2	2	0	2	8
(C6) $\ \mathbf{r}_k^p\ _{\mathbf{w}} \leq \tau\eta_{\text{RF}}^{\mathbf{w},p}, \forall p$	2	2	2	1	1	8

**5. Conclusion.** In this study, we have presented three new stopping criteria and compared the proposed criteria with several existing stopping criteria for the conjugate gradient algorithm within the context of high-order finite elements for solving the Poisson equation.

Criterion (C4) compares the error indicator  $\eta_{\text{BDM}}$  to the estimate of the algebraic error. The indicator  $\eta_{\text{BDM}}$  is computationally less expensive than  $\eta_{\text{BDM}}$ , and the associated stopping criterion is more robust than  $\eta_{\text{BDM}}$  criterion.

Criterion (C5) compares error indicator  $\eta_{\text{RF}}^{\mathbf{w}}$  to the weighted norm of the residual. The indicator is a natural upper bound for the weighted norm of the residual without involving any unknown constants. This criterion, which closely relies on the residual, offers advantages over criteria based on algebraic error estimation and a posteriori error estimation. It eliminates the difficulty of selecting an appropriate delay parameter in algebraic error estimation and has a more favorable computational cost. Moreover, it is robust with respect to the mesh size, the polynomial degree, and the shape regularity of the mesh.

Thirdly, we proposed a subdomain-based criterion (C6) for solving Poisson problems with highly variable piecewise constant coefficients. This stopping criterion terminates when the criterion is individually satisfied for each subdomain. It is the only tested criterion that ensures reliable termination for Example 4.3.2 with highly variable coefficients in the absence of a good preconditioner or deflation.

For problems with highly variable piecewise constant coefficients, criteria (C1), (C3), (C4), and (C5) recommend termination at a reasonable iteration for Example 4.3.1, but they are not reliable for Example 4.3.2. In such cases, criterion (C6) is used instead. However, it remains unclear when it is necessary to switch to the subdomain-based criterion. Further investigation is

planned for future work. Additionally, we plan to extend these criteria to more general problems, such as problems with continuous variable coefficients and mixed problems. Furthermore, it is natural to consider applying these criteria to nonconforming finite element methods.

#### Appendix A. Error indicators in subdomains.

An element is defined as an overlap element if at least one of its edges lies on the interface of  $\Omega_1$ ,  $\Omega_2$ , or  $\Omega_3$ . An element is an interior element if the element and all its edges are located in the interior of  $\Omega_1$ ,  $\Omega_2$ , or  $\Omega_3$ . An element is an exterior element if it is neither an overlap nor an interior element. The nodes that are present in the overlap elements are referred to as overlap nodes, and the set of all overlap nodes is represented by  $\mathcal{S}_o$ . Conversely,  $\mathcal{S}_i$  represents the set of nodes that belong to the interior elements but not the overlap elements. Similarly,  $\mathcal{S}_e$  denotes the set of nodes that belong to the exterior elements but not the overlap elements.

Since  $\|u - u_h^k\|_E$  is the sum of errors on all elements, we can define  $\|u - u_h^k\|_{E,i}$ ,  $\|u - u_h^k\|_{E,o}$ , and  $\|u - u_h^k\|_{E,e}$  as the sum of errors on all elements in the interior subdomain, overlap subdomain, and exterior subdomain, respectively. We define the subdomain algebraic errors in a similar manner.

On the other hand,  $\eta_{\text{RF}}$  and the linear residual are based on nodes, rather than elements. We define a diagonal matrix  $\mathbf{M}_o \in \mathbb{R}^{N_s \times N_s}$  to represent the mask of overlap nodes  $\mathcal{S}_o$  where diagonal entries are defined as

$$(\mathbf{M}_o)_{ii} = \begin{cases} 1, & x_i \in \mathcal{S}_o \\ 0, & \text{elsewhere.} \end{cases}$$

Likewise, we define matrices  $\mathbf{M}_i$  and  $\mathbf{M}_e$  for the interior subdomain and the exterior subdomain, respectively. We denote the restriction of  $\eta_{\text{RF}}$  in the overlap subdomain by  $\eta_{\text{RF}}^o$

$$\eta_{\text{RF}}^{\mathbf{w},o} := \|\mathbf{M}_o \mathbf{R}_k\|_{\mathbf{w}} + \|\mathbf{M}_o \mathbf{F}_k\|_{\mathbf{w}}.$$

The residual in the overlap subdomain is defined as

$$\mathbf{r}_k^o = \mathbf{M}_o \mathbf{r}_k.$$

Analogously, we define  $\eta_{\text{RF}}^i$  and  $\mathbf{r}_k^i$  for the interior subdomain,  $\eta_{\text{RF}}^e$  and  $\mathbf{r}_k^e$  for the exterior subdomain. The subdomain-based stopping criterion is:

$$\|\mathbf{r}_k^i\|_{\mathbf{w}} \leq \tau \eta_{\text{RF}}^{\mathbf{w},i}, \quad \|\mathbf{r}_k^e\|_{\mathbf{w}} \leq \tau \eta_{\text{RF}}^{\mathbf{w},e}, \quad \text{and} \quad \|\mathbf{r}_k^o\|_{\mathbf{w}} \leq \tau \eta_{\text{RF}}^{\mathbf{w},o}.$$

#### REFERENCES

- [1] A. AMRITKAR, E. DE STURLER, K. ŚWIRYDOWICZ, D. TAFTI, AND K. AHUJA, *Recycling Krylov subspaces for CFD applications and a new hybrid recycling solver*, J. Comput. Phys., 303 (2015), pp. 222–237, <https://doi.org/10.1016/j.jcp.2015.09.040>.
- [2] M. ARIOLI, *A stopping criterion for the conjugate gradient algorithm in a finite element method framework*, Numer. Math., 97 (2004), pp. 1–24, <https://doi.org/10.1007/s00211-003-0500-y>.
- [3] M. ARIOLI, E. H. GEORGIOULIS, AND D. LOGHIN, *Stopping criteria for adaptive finite element solvers*, SIAM J. Sci. Comput., 35 (2013), pp. A1537–A1559, <https://doi.org/10.1137/120867421>.
- [4] M. ARIOLI, J. LIESEN, A. MIĘDLAR, AND Z. STRAKOŠ, *Interplay between discretization and algebraic computation in adaptive numerical solution of elliptic PDE problems*, GAMM Mitt., 36 (2013), pp. 102–129, <https://doi.org/10.1002/gamm.201310006>.
- [5] M. ARIOLI, D. LOGHIN, AND A. J. WATHEN, *Stopping criteria for iterations in finite element methods*, Numer. Math., 99 (2005), pp. 381–410, <https://doi.org/10.1007/s00211-004-0568-z>.
- [6] I. BABUŠKA, R. DURÁN, AND R. RODRÍGUEZ, *Analysis of the efficiency of an a posteriori error estimator for linear triangular finite elements*, SIAM J. Numer. Anal., 29 (1992), pp. 947–964, <https://doi.org/10.1137/0729058>.
- [7] I. BABUŠKA, L. PLANK, AND R. RODRÍGUEZ, *Quality assessment of the a-posteriori error estimation in finite elements*, Finite Elem. Anal. Des., 11 (1992), pp. 285–306, [https://doi.org/10.1016/0168-874X\(92\)90011-Z](https://doi.org/10.1016/0168-874X(92)90011-Z).
- [8] I. BABUŠKA AND W. C. RHEINBOLDT, *Error estimates for adaptive finite element computations*, SIAM J. Numer. Anal., 15 (1978), pp. 736–754, <https://doi.org/10.1137/0715049>.
- [9] R. E. BANK AND J. XU, *Asymptotically exact a posteriori error estimators, part I: Grids with superconvergence*, SIAM J. Numer. Anal., 41 (2003), pp. 2294–2312, <https://doi.org/10.1137/S003614290139874X>.
- [10] P. BASTIAN AND B. RIVIÈRE, *Superconvergence and  $H(\text{div})$  projection for discontinuous Galerkin methods*, Int. J. Numer. Methods Fluids, 42 (2003), pp. 1043–1057, <https://doi.org/10.1002/flid.562>.

- [11] C. BERNARDI AND R. VERFÜRTH, *Adaptive finite element methods for elliptic equations with non-smooth coefficients*, Numer. Math., 85 (2000), pp. 579–608, <https://doi.org/10.1007/PL00005393>.
- [12] M. BOLTEN, E. DE STURLER, C. HAHN, AND M. L. PARKS, *Krylov subspace recycling for evolving structures*, Comput. Methods Appl. Mech. Eng., 391 (2022), p. 114222, <https://doi.org/10.1016/j.cma.2021.114222>.
- [13] Z. CAI, C. HE, AND S. ZHANG, *Improved ZZ a posteriori error estimators for diffusion problems: Conforming linear elements*, Comput. Methods Appl. Mech. Eng., 313 (2017), pp. 433–449, <https://doi.org/10.1016/j.cma.2016.10.006>.
- [14] Z. CAI AND S. ZHANG, *Robust equilibrated residual error estimator for diffusion problems: Conforming elements*, SIAM J. Numer. Anal., 50 (2012), pp. 151–170, <https://doi.org/10.1137/100803857>.
- [15] C. CARSTENSEN AND S. BARTELS, *Each averaging technique yields reliable a posteriori error control in FEM on unstructured grids. Part I: Low order conforming, nonconforming, and mixed FEM*, Math. Comp., 71 (2002), pp. 945–969, <https://doi.org/10.1090/S0025-5718-02-01402-3>.
- [16] C. CARSTENSEN AND S. A. FUNKEN, *Fully reliable localized error control in the FEM*, SIAM J. Sci. Comput., 21 (1999), pp. 1465–1484, <https://doi.org/10.1137/S1064827597327486>.
- [17] C. CARSTENSEN AND C. MERDON, *Estimator competition for Poisson problems*, J. Comp. Math., (2010), pp. 309–330, <https://doi.org/10.4208/jcm.2009.10-m1015>.
- [18] Z. DOSTÁL, *Conjugate gradient method with preconditioning by projector*, Int. J. Comput. Math., 23 (1988), pp. 315–323, <https://doi.org/10.1080/00207168808803625>.
- [19] A. ERN AND M. VOHRALÍK, *Adaptive inexact Newton methods with a posteriori stopping criteria for nonlinear diffusion PDEs*, SIAM J. Sci. Comput., 35 (2013), pp. A1761–A1791, <https://doi.org/10.1137/120896918>.
- [20] A. ERN AND M. VOHRALÍK, *Polynomial-degree-robust a posteriori estimates in a unified setting for conforming, nonconforming, discontinuous Galerkin, and mixed discretizations*, SIAM J. Numer. Anal., 53 (2015), pp. 1058–1081, <https://doi.org/10.1137/130950100>.
- [21] G. H. GOLUB AND G. MEURANT, *Matrices, moments and quadrature II; how to compute the norm of the error in iterative methods*, BIT Numer. Math., 37 (1997), pp. 687–705, <https://doi.org/10.1007/BF02510247>.
- [22] G. H. GOLUB AND G. MEURANT, *Matrices, moments and quadrature with applications*, vol. 30, Princeton University Press, 2009, <https://doi.org/10.1515/9781400833887>.
- [23] M. R. HESTENES AND E. STIEFEL, *Methods of conjugate gradients for solving linear systems*, J. Res. Natl. Bur. Stand., 49 (1952), pp. 409–436.
- [24] P. JIRÁNEK, Z. STRAKOŠ, AND M. VOHRALÍK, *A posteriori error estimates including algebraic error and stopping criteria for iterative solvers*, SIAM J. Sci. Comput., 32 (2010), pp. 1567–1590, <https://doi.org/10.1137/08073706X>.
- [25] J. M. MELENK AND B. I. WOHLMUTH, *On residual-based a posteriori error estimation in hp-FEM*, Adv. Comput. Math., 15 (2001), pp. 311–331, <https://doi.org/10.1023/A:1014268310921>.
- [26] G. MEURANT, *Numerical experiments in computing bounds for the norm of the error in the preconditioned conjugate gradient algorithm*, Numer. Algorithms, 22 (1999), pp. 353–365, <https://doi.org/10.1023/A:1019179412560>.
- [27] G. MEURANT, *The Lanczos and conjugate gradient algorithms: from theory to finite precision computations*, SIAM, 2006, <https://doi.org/10.5555/1177249>.
- [28] G. MEURANT, J. PAPEŽ, AND P. TICHÝ, *Accurate error estimation in CG*, Numer. Algorithms, 88 (2021), pp. 1337–1359, <https://doi.org/10.1007/s11075-021-01078-w>.
- [29] G. MEURANT AND P. TICHÝ, *On computing quadrature-based bounds for the A-norm of the error in conjugate gradients*, Numer. Algorithms, 62 (2013), pp. 163–191, <https://doi.org/10.1007/s11075-012-9591-9>.
- [30] L. MOTTA MELLO, E. DE STURLER, G. PAULINO, AND E. C. NELLI SILVA, *Recycling Krylov subspaces for efficient large-scale electrical impedance tomography*, Comput. Methods Appl. Mech. Engrg., 199 (2010), pp. 3101–3110, <https://doi.org/10.1016/j.cma.2010.06.001>.
- [31] R. A. NICOLAIDES, *Deflation of conjugate gradients with applications to boundary value problems*, SIAM J. Numer. Anal., 24 (1987), pp. 355–365.
- [32] J. T. ODEN, L. DEMKOWICZ, W. RACHOWICZ, AND T. A. WESTERMANN, *Toward a universal hp adaptive finite element strategy, part 2. a posteriori error estimation*, Comput. Methods Appl. Mech. Eng., 77 (1989), pp. 113–180, [https://doi.org/10.1016/0045-7825\(89\)90130-8](https://doi.org/10.1016/0045-7825(89)90130-8).
- [33] J. PAPEŽ, U. RÜDE, M. VOHRALÍK, AND B. WOHLMUTH, *Sharp algebraic and total a posteriori error bounds for h and p finite elements via a multilevel approach. Recovering mass balance in any situation*, Comput. Methods Appl. Mech. Eng., 371 (2020), p. 113243, <https://doi.org/10.1016/j.cma.2020.113243>.
- [34] J. PAPEŽ, Z. STRAKOŠ, AND M. VOHRALÍK, *Estimating and localizing the algebraic and total numerical errors using flux reconstructions*, Numer. Math., 138 (2018), pp. 681–721, <https://doi.org/10.1007/s00211-017-0915-5>.
- [35] M. PETZOLDT, *Regularity and error estimators for elliptic problems with discontinuous coefficients*, PhD thesis, 2001, <https://doi.org/10.17169/REFUBIUM-9770>.
- [36] M. PICASSO, *A stopping criterion for the conjugate gradient algorithm in the framework of anisotropic adaptive finite elements*, Commun. Numer. Methods Eng., 25 (2009), pp. 339–355, <https://doi.org/10.1002/cnm.1120>.
- [37] Y. SAAD, M. YEUNG, J. ERHEL, AND F. GUYOMARC'H, *A deflated version of the conjugate gradient algorithm*, SIAM J. Sci. Comput., 21 (2000), pp. 1909–1926, <https://doi.org/10.1137/S1064829598339761>.
- [38] K. M. SOODHALTER, E. DE STURLER, AND M. E. KILMER, *A survey of subspace recycling iterative methods*, GAMM Mitt., 43 (2020), p. e202000016, <https://doi.org/10.1002/gamm.202000016>.
- [39] Z. STRAKOŠ AND P. TICHÝ, *On error estimation in the conjugate gradient method and why it works in finite precision computations*, Electron. Trans. Numer. Anal., 13 (2002), pp. 56–80.
- [40] A. VEESER AND R. VERFÜRTH, *Explicit upper bounds for dual norms of residuals*, SIAM J. Numer. Anal.,

- 47 (2009), pp. 2387–2405, <https://doi.org/10.1137/080738283>.
- [41] S. WANG, E. D. STURLER, AND G. H. PAULINO, *Large-scale topology optimization using preconditioned Krylov subspace methods with recycling*, Int. J. Numer. Methods Eng., 69 (2007), pp. 2441–2468, <https://doi.org/10.1002/nme.1798>.
- [42] T. WARBURTON, *An explicit construction of interpolation nodes on the simplex*, J. Eng. Math., 56 (2006), pp. 247–262, <https://doi.org/10.1007/s10665-006-9086-6>.
- [43] Z. ZHANG AND A. NAGA, *A new finite element gradient recovery method: superconvergence property*, SIAM J. Sci. Comput., 26 (2005), pp. 1192–1213, <https://doi.org/10.1137/S1064827503402837>.
- [44] O. C. ZIENKIEWICZ AND J. Z. ZHU, *A simple error estimator and adaptive procedure for practical engineering analysis*, Int. J. Numer. Methods Eng., 24 (1987), pp. 337–357, <https://doi.org/10.1002/nme.1620240206>.
- [45] O. C. ZIENKIEWICZ AND J. Z. ZHU, *The superconvergent patch recovery and a posteriori error estimates. Part 1: The recovery technique*, Int. J. Numer. Methods Eng., 33 (1992), pp. 1331–1364, [https://doi.org/10.1016/0045-7825\(92\)90023-D](https://doi.org/10.1016/0045-7825(92)90023-D).